

**Description of seafloor sediment and preliminary  
geo-environmental report, Shelikof Strait, Alaska**

**by**

**Monty A. Hampton, Kris H. Johnson,  
Michael E. Torresan, and William J. Winters**

**U.S. Geological Survey  
Open-File Report 81-1133**

**This report is preliminary and has not been reviewed for conformity with U.S. Geological Survey editorial standards and stratigraphic nomenclature. Any use of trade names is for descriptive purposes only and does not imply endorsement by the USGS.**

## INTRODUCTION

Shelikof Strait, situated between the Kodiak island group and the Alaska Peninsula (Fig. 1), is included in OCS oil and gas lease area 60. Environments' geologic studies are being conducted by the U.S. Geological Survey prior to the scheduled September 1981 sale date. Seismic-reflection records, collected with 40- to 95-cm<sup>3</sup> airgun, 800-joule minisparker, 800-joule boomer, and 3.5- and 12-kilohertz systems and covering over 6,400 km of trackline have been examined to identify geologic conditions at or below the seafloor that might affect petroleum operations. Of the total trackline distance, 865 km were collected in June 1980 aboard the Geological Survey's ship R/V S.P. LEE. The remainder were collected by Nekton Inc. in 1979, under contract to the USGS (Fig. 2). Sediment samples were collected at 42 stations on the June 1980 cruise for geological and geotechnical analysis (Fig. 2).

The purpose of this report is to present physical and chemical measurements that have been made on sediment samples and to give a preliminary geo-environmental assessment of Shelikof Strait, based on presently completed analyses of the geophysical records and sediment samples.

## SETTING

Shelikof Strait marks the location of a northeast-trending structural trough, forming an inner forearc basin (von Huene, 1979) that is located near the convergent margin of the North America plate where it is being underthrust by the Pacific plate. The major tectonic feature is a clearly defined Benioff zone, located at a depth of just less than 100 km beneath the strait (Pulpan and Kienle, 1979).

The Gulf of **Alaska** - Aleutian region, which includes sale area 60, is one of the most seismically active on earth and accounts for about 7 percent of the annual worldwide release of seismic energy; mostly in the form of large earthquakes (greater than magnitude 6). Since recording of large earthquakes began in 1902, at least 95 potentially destructive events (**M>6**) have occurred in the vicinity of **Shelikof** Strait. Recurrence intervals of major earthquakes (**M>7.5**) within a given area along the Gulf of Alaska - Aleutian system have been estimated to be between a maximum of 800 years (**Plafker** and Rubin, 1967) and a minimum of 33 years (Sykes, 1971).

At least 12 volcanoes classified as active (within historic time) or recently active (<10,00 yr) are located along the Alaska Peninsula adjacent to the strait (Powers, 1958). The volcanoes are andesitic in composition and are subject to violent eruptions, as exemplified by the Katmai event of 1912, which expelled more than 25 km<sup>3</sup> of ash (Wilcox, 1959). The most recent eruption was that of Mt. Augustine in 1976 in nearby lower Cook Inlet.

Onshore geology and sparse deep seismic-reflection data indicate that many of the major geologic features of lower Cook Inlet extend into Shelikof Strait. These features include less than 2 km of Cenozoic and an undertermined thickness of Mesozoic strata, the Alaska - Aleutian Range batholith, and the Border Ranges fault (Magoon et al., 1979). Bedrock within the strait is covered by a blanket of relatively undeformed Quaternary glacial and marine sedimentary deposits.

### BATHYMETRY

The bathymetry of **Shelikof** Strait is shown in Figure 3. The map was prepared by hand-picking depths from 3.5- and 12-kilohertz profiles along all

tracklines shown in Figure 2, correcting depths to mean lower low water, computer posting and contouring, and manually smoothing the final product.

The seafloor of **Shelikof** Strait consists of a gently southwest-sloping central platform bordered by narrow marginal channels adjacent to the Kodiak islands and the Alaska Peninsula. Water depths in the northeast part are generally less than 200 m whereas those in the southwest generally exceed 200 m and can be as much as 300 m. Superimposed on the platform are some local highs and lows with as much as 100 m relief. Along the axes of the marginal channels are several closed depressions of up to 100 m relief.

#### SHALLOW STRUCTURES

Figure 4 shows trends of shallow structures. Faults were identified in airgun, minisparker and **uniboom** records by the presence of offset strata and hyperbolic reflections. Only faults that disrupt sediment above bedrock were mapped, and distinction is made between those that intersect the seafloor and those that terminate below it. Fold axes were taken from the map prepared by Hoose and Whitney (1980).

Most major structures trend parallel to the axis of the strait, perpendicular to the direction of plate convergence. Faults that offset the seafloor or extend above bedrock into unconsolidated sediment occur along both margins of the strait. Faults in the central part of the strait cause as much as 100 m offset of the seafloor and produce **horst** and graben structures seen in some seismic reflection records (Fig. 5).

Shallow bedrock folds are asymmetric, with vergence toward the northwest on the Kodiak Island side of the strait and toward the southeast on the Alaska Peninsula side (Hoose and Whitney, 1980). Most **folds** are truncated at the unconformable contact with overlying unconsolidated sediment.

## SEDIMENT

**Stratigraphy:** Sedimentary deposits of presumed Pleistocene and Holocene age overlie an irregular unconformity above Tertiary and older sedimentary bedrock. Thickness of unconsolidated sediment, measured from airgun, minisparker, and **uniboom** records, is generally about 100 **ms** of two-way acoustic penetration in the northeastern half of the study **area** and increases abruptly in the southwestern half to values exceeding 1000 **ms** (Fig. 6; see also Whitney et al., 1980 **a,b**). The thickening reflects a deepening of the unconformity. Interpretations of the seismic stratigraphy by Whitney et al. (1980 **a,b**), Hoose et al. (1980), and Holden (1980) reveal that the section above the unconformity comprises three sedimentary units: a lowermost (Pleistocene?) unit that fills the bedrock depression in the southwest half of the area and reaches thicknesses of more than 500 m, a lower Holocene unit generally about 100 m thick that overlies the unconformity in the northeast and the Pleistocene unit in the southwest, and an upper Holocene unit generally less than 20 m thick that covers most of the seafloor.

High-resolution seismic reflection records show that the platform area on the seafloor of **Shelikof** Strait represents the surface of a southwesterly prograding sediment body. This sediment body pinches out laterally across the strait to form the gently sloping seaward walls of the **marginal** channels (Fig. 7). The steep, landward channel **walls** appear to be fault scarps in some places, but more typically are **the** depositional surface of sediment derived from Pleistocene glaciers or the adjacent landmasses (Alaska Peninsula and Kodiak islands). Therefore, the channels are not erosional in origin but instead represent areas **of** little modern sediment accumulation. In fact, the overall sedimentary environment of **Shelikof** Strait apparently is **depositional**,

with no evidence of the erosion and large-scale reworking common nearby in Cook Inlet (Bouma et al., 1978) and on Kodiak Shelf (Hampton et al., 1979). Sedimentation reflects the dominantly **barotropic** flow of ocean water that enters the northeast end of the strait from Cook Inlet and the Gulf of Alaska (Schumacher et al., 1978; Muench and Schumacher, 1980).

Textures: Sedimentary textures were measured by sieving and pipetting into four size **classes:** coarse (>2 mm), sand (2-0.062 mm), **silt** (0.062-0.004 mm), and clay (<0.004 mm). Textures of **surficial** sediment grade uniformly down the strait from muddy sand at the northeast end to slightly sandy mud at the southwest end (Figs. 8,9), indicating progressive sorting by present-day transporting currents. A general fining across the strait, toward the southeast, exists in the southwestern half of the study area.

Index physical properties: **Geotechnical** index properties have been determined for many of the sediment cores. These include vane shear strength, sensitivity, water content, grain specific gravity, and plasticity (**Atterberg** limits) (Table 1).

Vane shear tests were performed with a motorized device at a rotation rate of **90°/min.** The vane was **1/2 inch** diameter and **1/2 inch high**, inserted into the sediment to a depth twice **the** height of the vane.

Peak undisturbed strengths and remolded strengths were measured. On board ship, vane shear tests were performed at the ends of 1-m core sections immediately after recovery. The axis of vane rotation was parallel to the core axis in these tests. In the laboratory, within two weeks after termination of the cruise, core sections were split longitudinally and vane shear tests were performed at 20-cm intervals with the axis of vane rotation perpendicular to core axes. Replicate measurements were made on matching

halves of some **cores**. **Some** tests were performed using a torque cell to measure resistance to vane rotation; others were run using a spring. Peak vane shear strengths ( $S_u$ ) generally increase toward the northeast (Fig. 10, Table 1 ), reflecting the increase in grain size. Most of the sediment can be classified as **very** soft ( $S_u < 12$  kilopascals), but some is soft ( $12\text{kPa} < S_u < 24\text{kPa}$ ) to medium ( $24\text{kPa} < S_u < 48\text{kPa}$ ). These values are within typical ranges for **shallow** marine sediment (e.g., Keller, 1968, 1974).

$S_u$  values ideally increase down core, reflecting an increase in effective stress and a decrease in water content. This is true for most cores in **Shelikof** Strait, except for cores at stations 530 and 550, where strengths decrease. This strength reduction down core may be due to cementation of the near-surface sediment or an internal fabric effect (e.g., Bennett et al. , 1977).

Replicate vane tests made on matching core halves fall into two groups. In the first, the replicate tests were both made with the torque-cell apparatus, whereas in the second, one test was made with the torque cell and the other was made using a spring to measure resistance to vane rotation. Peak undisturbed strengths and remolded strengths were measured. The results are summarized in Table 2. Differences between replicate measurements are expressed as  $V$ , the coefficient of variation (difference between the two measurements, divided by the mean, expressed as a percent). As shown in the table, the range of  $V$  is **large (0-113%)**, **but the averages** and standard deviations are moderate. The mean of all replicate torque-cell measurements is 24% for both peak undisturbed strengths and remolded strengths. Standard deviations are 20% and 22%, respectively.  $V$ -values for the torque-cell/spring replicate measurements have a grand mean of 22% for peak strengths and 26% for remolded strengths, with standard deviations of 16% and 26%, respectively.

Vane shear strength tests made at the ends of core sections measure strength along a vertical cylindrical surface within the sediment, whereas tests made on split core sections measure strength on a cylindrical surface whose axis is perpendicular to the core axis and contains planes in all directions from vertical to horizontal. Thus, end-core tests measure strength on planes that are of different orientation than those on which strength is measured in a split-core test. Some difference in end-core and split-core values might be expected, because strength can be anisotropic in sediments. Moreover, Bjerrum (1973) demonstrated an inverse relation between the magnitude of anisotropy (in a horizontal plane versus a vertical plane) and plasticity index using several different natural clays. In order to make a similar analysis of Shelikof Strait sediment, some adjustments of the data were made to account for the fact that end-core and split-core measurements were not taken at the same levels in cores. Namely, linear regression equations were derived for both the undisturbed and remolded split-core strengths as a function of water content for several cores with abundant vane strength data (Table 3). No anisotropy should exist for remolded samples, so the difference between the remolded end-core measurements and the corresponding split-core regression line was considered to represent the real deviation from linearity, reflecting variations within the sediment column that affect strength.

This difference, which also includes some experimental error, should be inherent in the undisturbed strength values, too, so the deviation computed for the remolded strength was subtracted from the corresponding undisturbed strength. Then, this corrected value was divided into the corresponding (equal water content) value on the undisturbed, split-core regression line to give a measure of anisotropy. As shown in Fig. 11, nearly all split-tote

values exceed those from ends of cores, giving an anisotropy greater than one. No correlation with Bjerrum's (1973) experimental curve is evident, however.

Values of sensitivity,  $S$ , the ratio of undisturbed strength to remolded strength, fall in the low ( $1 < S < 2$ ) to quick ( $S > 16$ ) range (Terzaghi and Peck, 1948), with most being classified as medium sensitive ( $2 < S < 4$ ) (Table 1). The coarser sediment in the northeastern area tends to have higher sensitivity values (Fig. 12, Table 1).

Water content (as a percentage of dry sediment weight) generally decreases to the northeast, inversely correlating with grain size (Fig. 13, Table 1). Moreover, water contents increase across the strait, from the Alaska Peninsula to Kodiak Island. Values in the northeast are perhaps low for marine sediment, but most are in the range of measurements taken elsewhere (Keller, 1968, 1974).

Atterberg limits describe the plasticity of sediment, in terms of the liquid limit (water content separating plastic and liquid behavior) and plastic limit (water content separating solid and plastic behavior). Useful derivatives are the plasticity index (difference between the liquid and plastic limits), and the liquidity index (position of the natural water content relative to the liquid and plastic limits). Certain trends in plasticity are evident in Shelikof Strait. Liquid limit, plastic limit, and plasticity index increase down the strait toward the southwest, and also generally across the strait, toward the southeast (Table 1, Figs. 14, 15, 16). These properties also generally increase with decreasing mean grain size (Figs. 17, 18, 19), although the data for plastic limit are quite scattered. Plastic limits are less variable than liquid limits, which is typically the (Mutchell, 1976; Richards, 1962).

Correlations have been made between liquid limit ( $w_L$ ) and compressibility (Herrmann et al., 1972; Skempton, 1944). The majority of Shelikof Strait samples fall within the medium ( $30 < w_L < 50$ ) and high ( $w_L > 50$ ) compressibility ranges.

All measured liquidity indices in Shelikof Strait are greater than 1 (Table 1) which is usual for near-seafloor marine sediment. Most cores show a decrease in liquidity index with depth, reflecting the decrease in water content. Sediment with a liquidity index greater than one behave as a liquid when remolded.

A plot of liquid limit versus plasticity index - termed a plasticity chart (Casagrande, 1948) - shows a trend parallel to the A-line that divides basic soil types (Fig. 20). Most sediments from Shelikof Strait plot below the A-line, which is typical of inorganic silts and silty clays. The linear trend of data points is expected for samples taken throughout the same sedimentary deposit (Terzaghi, 1955; Richards, 1962).

Other index properties obtained include grain specific gravity, bulk sediment density (assuming 100% saturation), void ratio, and porosity (Table 1). Sediment density decreases toward the southwest, whereas void ratio and porosity increase. Across the strait, toward the southeast, sediment density decreases, and void ratio and porosity increase. Grain specific gravity varies over a small range, with most values between 2.65 and 2.84. No trends are apparent. Typical variations with depth in cores are as follows: void ratio and porosity decrease, bulk sediment density increases, and grain density shows no trend.

Carbon: Dry-weight percentages of carbonate and organic carbon were measured for **subsamples** taken from the upper 2 to 3 cm of cores at 31

locations in Shelikof Strait (Figs. 21, 22). Carbon-carbonate analysis was performed on a LECO model **WR-12** carbon determinator with induction furnace and acid digester. **Subsamples** were first freeze-dried, ground to a fine powder, and stored in a desiccator. Total carbon was measured using the induction furnace, and carbonate carbon was determined with the acid digester. Organic carbon content is calculated as the difference between total carbon and carbonate carbon contents. The reported values of organic carbon and carbonate carbon represent the average of 3 analyses from each core.

**Surficial** sediment of Shelikof Strait is characterized by low to intermediate contents of organic carbon, compared to other marine areas (**Bordovskiy**, 1965, 1969; Gardner, 1980; Lisitzin, 1972; Rashid and Brown, 1975). **Values** range from 0.10% to 3.16%, averaging 0.82%. Most values are between 0.40% and 1.50%.

Organic carbon content generally increases down the strait toward the southwest, as well as across the strait toward the southeast. These values vary inversely with grain size (Fig. 23). Correlations with other physical properties are shown in Figs. 24 through 28. Organic carbon content correlates positively with water content and plasticity index, whereas general inverse correlations are found with vane shear strength and sensitivity. Data are too scattered to define a correlation between organic carbon content and liquidity index. Correlations similar to those described above have been reported by others for low organic-carbon content sediments (**Bordovskiy**, 1965, 1969; Bush and Keller, 1981; **Keller et al.**, 1979, **Lisitzin**, 1972; **Mitchell**, 1976; **Odell et al.**, 1960).

Percent carbonate carbon is typically low in Shelikof Strait sediment, varying between 0.84% and **38.76%** (average = **2.96%**)(**Fig. 22**). Most values are

**less than 3.50%.** **Two** locations (535 and 553) with anomalously high values (21.67% and 38.76%, respectively) are near the boundary of the strait.

Clay mineralogy: Forty-four samples of **surficial** sediment were analyzed for clay mineralogy. Sample preparation and clay-mineral identification methods generally follow those presented by Hein et al. (1976). Samples were analyzed on a Picker high-angle x-ray diffractometer with a scintillation counter using nickel-filtered copper Ku radiation. Carbonate and organic carbon were removed from sediment samples with Morgan's solution (sodium acetate and glacial acetic acid diluted with distilled water) and 30% hydrogen peroxide, respectively.

The <2  $\mu\text{m}$  size fraction was separated by centrifugation. This clay-size fraction was Mg-saturated and mounted on glass slides (Gibbs, 1965). The mounts were **glycolated** and then heat-treated at 500°C for one hour. An x-ray **diffractogram** ( $2\theta = 3^\circ\text{-}140^\circ$ ) was taken following each of the above treatments.

The semiquantitative technique of measuring peak areas was used to calculate the relative clay-mineral percentages. **Biscaye's** (1965) peak area weighting factors of two for **chlorite-kaolinite**, four for **illite**, and one for smectite were used in calculating relative percentages. Percentages of chlorite relative to **kaolinite** were obtained from a slow scan of the  $24^\circ\text{-}26^\circ$   $2\theta$  diffractogram (**Biscaye, 1964**). Kaolinite was a minor component in these samples, making accurate determinations difficult. **Biscaye's** method showed no discernible **kaolinite** peak at  $24.88^\circ$   $2\theta$ . The chlorite values presented here include any **kaolinite** that may have been present but was not measurable. Duplicate samples and duplicate sample runs showed reproducibility within 5%.

**Illite** and chlorite are the dominant clay minerals in **Shelikof** Strait, averaging 52% and 42%, respectively (Figs. 29,30; Table 4). Mixed layer clay (mostly smectite) occurrence is minor and averages 6% (Fig. 31). The major gradients in clay mineral abundances occur across the strait, perpendicular to the axis. At the northeast boundary of the strait, however, gradients tend to become oblique to the axis. The highest values of **illite** and the lowest values of chlorite generally occur along the axis. Mixed layer clays occur more abundantly on the southeastern side of the strait compared to the northwestern side, and most abundantly at the northeast end of the strait.

The flow that transports clay minerals into **Shelikof** Strait derives mainly from Cook Inlet and from the northeastern Gulf of Alaska (Muench and Schumacher, 1980). Clay mineral suites from these areas, as well as from nearby Kodiak Shelf, have been described by Hein et al. (1979). Average compositions of these suites, as well the average from **Shelikof** Strait, are presented in Table 5. The clay mineral suite in **Shelikof** Strait most closely resembles that from Cook Inlet, but some contribution from the northeastern Gulf (i.e., Copper River) surely is present.

The relative enrichment of chlorite and depletion of **illite** along the margins of the strait may represent contributions of clay minerals from the adjacent landmasses. Alternatively, the segregation might reflect hydraulic sorting processes (Gibbs, 1977; **Knebel** et al., 1977). **Stratigraphic** evidence (i.e., the non-depositional channels) suggests that the margins of the strait are hydrodynamically high-energy areas, implying that clay minerals with relatively low settling velocities would be depleted, which apparently is the case. **Knebel** et al. (1977) demonstrated that chlorite and **kaolinite** in San Francisco Bay sediment is coarser than **illite**, and that hydraulic sorting

on the basis of size exists. The distribution of mixed layer clays in **Shelikof** Strait, present in relatively small amounts and presumably finer grained than the other clays, shows a sorting trend, but it is not clearly compatible with that shown by the other clays. Mixed-layer clay distribution suggests a source from Kodiak Shelf.

Gas: Sediment samples at 15 stations were **analysed** for light hydrocarbon gases (methane through butane), by K. Kvenvolden and T. Vogel. In general, gas concentrations were low (Table 6). Methane was approximately **30 microliters/liter ( $\mu\text{l/l}$ )** of wet sediment, ethane was about **100 nanoliters/liter ( $\text{nl/l}$ )**, propane was **100  $\text{nl/l}$** , and ethane was **80  $\text{nl/l}$** . Isobutane and n-butane were negligible.

One station showed anomalous gas concentrations. Sediment from station 539 exhibited large methane (**1600  $\mu$** ) and ethane (**946  $\text{nl/l}$** ) concentrations. The sample was unusual, because the methane/ethane + propane ratio was high ( $C_1/C_2 + C_3 = 1556$ ) indicating biogenic gas, and yet the ethane/ethene ratio was also high ( $C_2/C_{2:1} \approx 16$ ), suggesting a thermogenic source. Ethene is normally the same concentration or greater than that of ethane in biogenic gases, but due to the low concentrations of the other saturated hydrocarbons (propane, **iso-butane**, and n-butane), the gas at station 539 **can be** assumed **biogenic**.

#### ACOUSTIC ANOMALIES

Anomalous acoustic signatures exist in many **boomer** and **minisparker** records. Typically, they appear as unusually strong reflections, with abrupt terminations, within the unconsolidated sediment section. Reflectors below the anomaly are commonly obscured. A few instances where all reflectors

beneath the seafloor are totally obscured, with no evidence of strong reflectors, were also found.

Anomalies occur most commonly in the northeastern half of the strait, but **some also exist in the** southwest (Fig. 32). Many anomalies occur over steeply dipping bedrock strata and **anticlinal** crests that have been truncated by erosion (Fig. 33).

Acoustic anomalies are not **all** easy to distinguish, because a continuous gradation exists from normal acoustic returns, through subtle deviations from normal, to distinct anomalies. Instrument settings, such as filter frequencies and gain modes (TVG versus **AGC**), have an influence on the appearance of anomalies. It is commonly a matter of judgment what to identify as a true acoustic anomaly. Only distinct anomalies are mapped on Fig. 32.

Acoustic anomalies have been shown in other areas to be caused by gas charging (Nelson et al., 1978; Whelan et al., 1976; **Schubel, 1974**). A similar causative relationship has not been confirmed in **Shelikof Strait**, but it cannot be discounted. The occurrence of some anomalies over truncated **anticlines** and steeply inclined bedrock strata is consistent with an origin due to migrated gas, but the absence of significant concentrations of gas in cores and of water-column gas seeps in the seismic records argues against it, unless, of course, the gas is completely trapped and cannot leak to the surface. Alternatively, the anomalies may be due to change in lithology along stratigraphic horizons.

#### CRATERS

Seafloor craters occur over an area of approximately 1500 km<sup>2</sup> on the progradational platform in **Shelikof Strait** (Fig. 34). The craters appear on

seismic reflection profiles as small indentations, typically 50 m in diameter and less than 5 m deep (Fig. 35). Broad, low relief rims about 1 m high can be detected on some. In side-scanning sonar records, the craters are subtle features and circular *in plan* (P.J. Hoose, personal communication). The craters are similar in appearance to those found on the Scotian Shelf by King and MacLean (1970). Disruption of seismic reflectors cannot be detected beneath most craters. Moreover, nearly all craters occur on the present-day seafloor. Only a few examples of buried craters were found (Figs. 34 and 35), and most of these occur within a subbottom depth of 25 m.

Origin of the craters is unknown, but one possibility is venting of either gas or buried, liquefied sediment. The lack of disruption of seismic reflectors suggests a shallow source; less than a few meters. Gas venting is believed to cause craters in other places, such as in Norton Sound where a buried Pleistocene peaty mud is the source of gas (Nelson et al., 1979). No evidence of an organic-rich layer was detected in Shelikof Strait cores, and as mentioned above, measured contents of hydrocarbon gases are low. Furthermore, the location of acoustic anomalies, which are also believed typically to be related to gas (Nelson et al., 1978; Whelan et al., 1976; Schubel, 1974), are almost mutually exclusive of the locations of craters in Shelikof Strait.

There is an interesting correlation of the occurrence of craters with the subsurface extent of the thick Pleistocene(?) unit of Whitney et al. (1980a,b). The two are nearly coincident. But if the two features were related, some disturbance of the intervening 100 m or so of unconsolidated sediment would be expected, which is not the case.

Alternatively, craters might be formed by collapse or venting of buried liquefied sediment. In particular, a layer of Katmai ash blankets most of the strait and was encountered in many cores. At nearly all locations within the crater field, penetration of the gravity core was stopped at **subbottom** depths of less than 35 cm. Dart coring at one locality revealed a dense layer of ash about 15 cm thick at this depth. Perhaps this material and other ash layers were originally deposited in a loose state and have liquefied after burial, although this process does not account for the relief of the craters, which is much greater than the thickness of ash recovered in cores.

Liquefaction, if it has occurred, could have been caused by a severe earthquake such as the one in 1964. On the other hand, the area is too deep for storm-wave loading to cause liquefaction (e.g., Hampton et al., 1978).

#### SEDIMENT SLIDES

Examination of seismic reflection records shows that the seafloor of Shelikof Strait is nearly devoid of sediment slides. Only one instance of a slide mass was found (Figs. 4, 36), and it was derived from an adjacent fault scarp. The slide mass extends for about 100 m along one **trackline** and is less than 10 m thick.

Although most of the seafloor is flat, several steep slopes exist in **Shelikof** Strait. Name ly, the landward walls of the marginal channels and the large-offset fault scarps in the central part of the strait have declivities **that** commonly exceed the resolving capability of the seismic reflection system (about 15°) and maY locally approach vertical. Evidently, the sediment underlying these slopes is generally strong enough to resist the downslope driving forces of gravity and earthquake accelerations.

## ENVIRONMENTAL ASSESSMENT

The tectonic setting of **Shelikof** Strait, near **the** convergent margin of two major **lithospheric** plates, makes it subject to large earthquakes. The minimum recurrence interval of 33 years for a major earthquake that could affect the entire region might be exceeded by the lifetime of an oil-producing province, because the last major event was in 1964. So, although earthquakes cannot be predicted with confidence, seismic hazards are a valid concern for offshore development. Strong ground shaking, fault rupture, sediment displacement, and tectonic deformation have all been documented in nearby areas. Examination of the distribution of historic epicenters shows no **areal** concentrations (H. **Pulpan**, Univ. Alaska, personal communication), such as exist nearby on Kodiak Shelf (Hampton et al. , 1979), that would imply some areas are more susceptible to local seismic affects than others.

Violent volcanic explosions are also associated with the tectonic setting, and eruptions from the volcanoes on the Alaska Peninsula could cause problems such as substantial ash accumulations and acid rains. More destructive but local effects such as hot ash flows are not likely in most parts of the strait.

The faults in **Shelikof** Strait that offset the seafloor imply recent activity and the probability of more to come. The seafloor offset (100 m) of some faults in the central part of the strait implies major movement in recent times. The short extent, irregular shape, and **horst-like** appearance of these faults suggest that perhaps they are caused by forces associated with localized uplift rather than being a direct result of regional compression.

The sedimentary environment of **Shelikof** Strait is **depositional**, with sandy material presently being deposited to the northeast and progressively

finer material accumulating to the southwest. Problems associated with scour or movement of large **bedforms**, a significant concern on Kodiak Shelf and in lower Cook Inlet, should not exist in **Shelikof Strait**. Accumulation of fine sediment does raise the possibility of pollutant storage on the seafloor, though. Pollutants introduced within the strait itself or in more diluted form from lower Cook Inlet and the northeastern Gulf of Alaska could be stored as contaminants on fine particles.

Seafloor sediment in **Shelikof Strait** exhibits physical properties (vane shear strength, water content, plasticity) similar to those of marine sediment elsewhere. Measurements of physical properties are useful for categorizing the shallow sediment types in the strait, but deeper samples and more sophisticated testing would be necessary for engineering design purposes. A few high values of sensitivity and compressibility were obtained, but most measurements of physical properties are in normal ranges for shallow marine sediment, and no unusual **geotechnical** problems are indicated. Deeper unconsolidated sediment apparently is stable, coarse-grained glacial debris. **Geotechnical** triaxial and consolidation testing now underway will give more detailed strength and consolidation information than is now available for the uppermost sedimentary units.

Sediment slides are uncommon in the strait; only one occurrence is known. Nevertheless, the steep slopes **along** fault scarps and also along the landward side of the marginal channels must be regarded as possible sites of local instability.

Indirect evidence for gas-charged sediment, in the form of acoustic anomalies, is especially common in the northeast part of the strait and warns that weak and unstable sediment, as well as high gas pressures, might be

present in the shallow subsurface. Low gas contents in cores (except one) and the absence of seeps from the seafloor, however, are inconsistent with the hypothesis of widespread gas-charged sediment.

The seafloor craters in the southwest area might also indicate the presence of gas-charged sediment, although the locations of craters is nearly exclusive of the locations of acoustic anomalies, which argues against this. A more likely explanation for the craters is sediment venting due to liquefaction. A source at depths of less than about 10 meters below the seafloor is likely for the liquefied layer, and therefore the venting may represent only a minor environmental concern.

#### ACKNOWLEDGMENT

This study was jointly funded by the U.S. Geological Survey and the Bureau of Land Management through interagency agreement with the National Oceanic and Atmospheric Administration, under which a multi-year program responding to needs of petroleum development of the Alaskan continental shelf is managed by the Outer Continental Shelf Environmental Assessment Program (OCSEAP) office.

REFERENCES CITED

- Bennett, R. H., Bryant, W. R., and Keller, G. H., 1977, Clay fabric and geotechnical properties of selected submarine sediment cores from the Mississippi Delta: NOAA Professional Paper 9, 86 p.
- Biscaye, P. E., 1964, Distinction between kaolinite and chlorite in recent sediments by x-ray diffraction: Am. Mineralogist, v. 49, p. 1281-1289.
- Biscaye, P. E., 1965, Mineralogy and sedimentation of Recent deep sea clay in the Atlantic Ocean and adjacent sea and oceans: Geol. Soc. America Bull., v. 76, p. 803-832.
- Bjerrum, L., 1973, Problems of soil mechanics and construction on soft clays and structurally unstable soils: Proceedings of the Eighth International Conference on Soil Mechanics and Foundation Engineering, v. 3, p. 111-159.
- Bordovskiy, O. K., 1965, Accumulation of organic matter in bottom sediments: Marine geology, v. 3, p. 33-82.
- Bordovskiy, O. K., 1969, organic matter of recent sediments of the Caspian Sea: Oceanology, v. 9, p. 799-807.

Bouma, A. H., Hampton, M. A., Rapoport, M. L., Whitney, J. W., Teleki, P. G., Orlando, R. C., and Torresan, M. E., 1978, Movement of sandwaves in lower Cook Inlet, Alaska: Preprints 10th Offshore Technology Conference, p. 2271-2284.

Bush, W. H., and Keller, G. H., 1981, The physical properties of Peru-Chile continental margin sediments - the influence of coastal upwelling in sediment physical properties: , in press.

Cassagrande, A. 1948, Classification and identification of soils: Transactions, American Soc. Civil Engineers, v. 113, p. 901-991.

Feely, R. A., and Massoth, G. J., 1981, Sources, composition, and transport of suspended particulate mater in lower Cook Inlet and northwestern Shelikof Strait, Alaska: in Bouma, A. H. (cd.), Geology of Lower Cook Inlet: U.S. Geological Survey Professional Paper, in press.

Gardner J. V., Dean, W. E., and Vallier, T. L., 1980, Sedimentology and geochemistry of surface sediments, outer continental shelf, southern Bering Sea: Marine Geology, v. 35, p. 299-329.

Gibbs, R. J., 1965, Error due to segregation in quantitative clay mineral x-ray diffraction mounting techniques: Am. Mineralogist, v. 50, p. 741-751.

Gibbs, R. J., 1977, Clay mineral segregation in the marine environment: Jour. Sedimentary Petrology, v. p. 237-243.

Griffin, J. J., and Goldberg, E. D., 1963, Clay-mineral distributions in the Pacific Ocean: in *The Sea--ideas and observations on progress in the study of the seas*, v. 3, *The earth beneath the sea and history*: Interscience Publishers, N.Y., p. 728-741.

Hampton, M. A., Bouma, A. H., Pulpan, H., and von Huene, R., 1979, **Geo-**environmental assessment of the Kodiak Shelf, western Gulf of Alaska: *Proceedings 11th Offshore Technology Conference*, p. 365-376.

Hampton, M. A., Bouma, A. H., Sangrey, D. A., Carlson, P. R., Molnia, B. F., and Clukey, E. C., 1978, Quantitative study of slope instability in the Gulf of Alaska: *Preprints 10th Offshore Technology Conference*, p. 2308-2318.

Hein, J. R., Bouma, A. H., Hampton, M. A., and Ross, R. C., 1979, Clay mineralogy, **fine-grained** sediment dispersal, and inferred current patterns, lower Cook Inlet and Kodiak Shelf: *Sedimentary Geology*, v. 24, p. 291-306.

Hein, J. R., Scholl, D. W., and Gutmacher, C. E., 1976, Neogene clay minerals of the far **NW** Pacific and southern Bering Sea: *Sedimentation and Diagenesis*: in **Bailey, S. W.** (ed.), *Proceedings of the International Clay Conference, 1975, Mexico City*. Applied Publishers, Ltd., **Wilmette, Ill.**, p. 71-80.

Herrmann, H. G., Rucker, **K.**, and **Babineau**, P. H., 1972, LOBSTER and FMS:

Devices for monitoring long-term seafloor foundation behavior: Nava 1  
Civil Engineering Laboratory, Technical Report R-775, 63 p.

**Holden**, K. D., 1980, **Isopach** map of upper Holocene marine sediments, outer  
continental shelf, **Shelikof** Strait, Alaska: U.S. Geological Survey Open-  
File Report 80-2032, 1 p.

Hoose, P. J., Holden, K. D., and Lybeck, L., 1980, **Isopach** map of Holocene  
marine sediments, outer continental **shelf, Shelikof** Strait, **Alaska:** Us.  
Geological Survey Open-File Report 80-2033, 1 p.

**Hoose**, P. J., and Whitney, J., 1980, Map showing selected geologic features on  
the outer continental shelf, **Shelikof** Strait, Alaska: U.S. Geological  
Survey Open-File Report 80-2035, 1 p.

Keller, G. H., 1968, Shear strength and other physical properties of sediments  
from some ocean basins: in Civil Engineering in the Oceans, New York,  
American Assoc. Civil Engineers, p. 391-417.

Keller, G. H., 1974, Marine **geotechnical** properties: interrelationships and  
relationships to depth of burial: in **Inderbitzen**, A. L. (cd.), Deep-Sea  
Sediments, New York, Plenum Press, p. 77-100.

Keller, G. H., Lambert, D. N., and Bennett, R. H., 1979, **Geotechnical** properties of continental slope deposits - Cape Hatteras to Hydrographer Canyon: *Sot. Economic Paleontologists and Mineralogists Special Publication 27*, p. 131-151.

King, L. H., and MacLean, B., 1970, Pockmarks on the Scotian Shelf: **Geol.** *Sot. America Bull.*, v. 81, p. 3141-3148.

**Knebel, H. J., Conomos, T. J., and Commeau, J. A.,** 1977, Clay-mineral variability in the suspended sediments of the San Francisco Bay System, California: *Jour. Sedimentary Petrology*, v. 47, p. 229-236.

Lisitzin, A. P., 1972, Sedimentation in the World Ocean: *Sot. Economic Paleontologists and Mineralogists Special Publication 17*, 218 p.

Magoon, L. B., **Bouma, A. H., Fisher, M. A.,** Hampton, M. A., Scott, E. W., and Wilson, C. L., 1979, Resource report for proposed OCS sale no. 60, lower Cook Inlet - **Shelikof** Strait, Alaska: U.S. Geological Survey Open-File Rept. 79-600, 38 p.

Mitchell, J. K., 1976, *Fundamentals of Soil Behavior*: New York, John Wiley and Sons, Inc., 422 p.

**Muench, R. D.,** and Schumacher, J. D, 1980, Physical oceanographic and meteorological conditions in the northwest Gulf of Alaska: NOAA Technical Memorandum ERL **PMEL-22**, 147 p.

- Nelson, C. H., Kvenvolden, K. A., and **Clukey**, E. C., 1978, Thermogenic gases in near-surface sediments in Norton Sound, Alaska: Preprints 10th Offshore Technology Conference, p. 2623-2633.
- Nelson, C. H., Thor, D. R., Sandstorm, M. W., and Kvenvolden, K. A., 1979, Modern biogenic gas-generated craters (sea-floor "pockmarks") on the Bering shelf, Alaska: **Geol. Soc. America Bull.**, v. 90, p. 1144-1152.
- Odell, R. T., **Thornburn**, T. H., and McKenzie, L. T., 1960, Relationships of Atterberg limits to some other properties of Illinois soils: Proceedings of the Soils Society of America, **v. 24**, p. 297-300.
- Plafker**, G., and Rubin, M., 1967, Vertical tectonic displacements in south-central Alaska during and prior to the great 1964 earthquake: Jour. Geosci. Osaka City Univ., p. 53-72.
- Powers, H. A., 1958, Alaska Peninsula - Aleutian Islands: in Williams, H. (ed.), Landscapes of Alaska, University of California Press, p. 61-75.
- Pulpan**, H., and Kienle, J., 1979, Western Gulf of Alaska seismic risk: Preprints 11th Offshore Technology Conference, p. 2209-2218.
- Rashid, M. A., and Brown, J. P., 1975, Influence of marine organic compounds on engineering properties of remolded sediment: Engineering Geology, v. 9, p. 141-154.

Richards, A. 1?., 1962, Investigation of deep-sea sediment cores, II. Mass physical properties: U.S. Navy **Hydrographic** Office Tech. Rept. 106, 146 p.

Schumacher, J. D., **Sillcox**, R., **Dreves**, D., and **Muench**, R. D., 1978, Winter circulation and hydrography over the continental shelf of the northwest Gulf of Alaska: NOAA Tech. Rept. ERL 404-PMEL 31.

**Schubel**, J. R., 1974, Gas bubbles and the acoustically impenetrable, or turbid, character of some marine sediments: in I. R. Kaplan (cd. ), Natural Gases in Marine Sediments, New York, **Plenum** Press, p. 275-298.

Skempton, A. W, 1944, Notes on the compressibility of clays: Geological Society of London, Quarterly Journal, v. 100, p. 119-135.

Sykes, L. R., 1971, Aftershock zones of great earthquakes, seismicity gaps, and earthquake prediction for Alaska and the Aleutians: Jour. Geophysical Research, v. 75, p. 8021-8041.

**Terzaghi**, K., 1955, Influence of geological factors on the engineering properties of sediments: Economic Geology, 50th Anniversary Volume 1905-1955, p. 557-618.

**Terzaghi**, K. , and Peck, R. B., 1948, Soil Mechanics in Engineering Practice: New York, John Wiley and Sons.

von **Huene, R., 1979**, Structure of the outer convergent margin off Kodiak Island, Alaska, from multichannel seismic records: in Watkins, J. S., **Montadert, L., and Dickerson, P. W., (eds.)**, Geological and Geophysical Investigations of Continental Margins, **AAPG** Memoir 29, Tulsa, American Association of Petroleum Geologists, p. 261-272.

Whelan, T., Coleman, J. M., Roberts, H. A., and **Suhayda, J. N., 1976**, The occurrence of methane in recent deltaic sediments and its effect on soil stability: International Assoc. Engineering Geologists Bull., no. 14, p. 55-64.

Whitney, J., Holden, K. D., and Lybeck, L., 1980a, **Isopach** map of Quaternary glacial-marine sediments, outer continental shelf, **Shelikof** Strait, Alaska: U.S. Geological Survey Open-File Report 80-2036, 1 p.

Whitney, J., **Hoose, P. J., Smith, L. M., and Lybeck, L., 1980b**, Geologic cross sections of the outer continental shelf, **Shelikof** Strait, Alaska: U.S. Geological Survey Open-File Report 80-2036, 1 p.

Wilcox, R. E., 1959, Some effects of recent volcanic ash falls with special reference to Alaska: U.S. **Geol. Survey Bull.**, no. 1028-N, p. 409-476.

Table 1. Physical properties of sediment cores.

Station	Latitude	Longitude	Water depth (m)	Depth in core (cm)	Grain size (weight percent)				Mean grain size $\phi$	Water content (%)	Wet bulk			Grain - Vaneshwan strength (k Pa)				Atterberg limits			
					coarse	sand	silt	clay			density (gm/cm <sup>3</sup> )	Void ratio	Porosity (%)	specific gravity	undisturbed	sensitized	liquid limit (%)	plastic limit (%)	plasticity index (%)	liquid-liquidity index	
50B	57° 1.01'N	155° 36.41'W	270	0	0	1	34	65	8.6												
				13	0	3	47	50	7.9	104.2	1.46	2.65	72.8	2.80	3.1	0.8	3.8	69	27	42	1.84
				21						106.2	1.48	2.92	74.5	2.81	5.0*	2.6*	1.9				
				35						105.1	1.48	2.89	74.3	2.81	4.9	0.9	5.4				
				55	0	2	44	54	8.0	88.9	1.55	2.47	71.2	2.84	8.2	2.1	4.0	70	40	30	1.63
				68											5.4	1.6	3.3				
				75						85.2	1.57	2.39	70.5	2.87	9.0	2.6	3.4				
				90											16.5	4.3	3.8				
				95						81.0	1.59	2.26	69.3	2.85	13.1	4.8	2.7				
				110	0	4	40	55	8.0	85.9	1.57	2.44	70.9	2.90	9.0	2.6	3.5	69	38	31	1.55
				121						66.4	1.64	1.76	63.8	2.71	4.2*	2.0*	2.0				
				130						82.9	1.58	2.33	70.0	2.88	11.6	4.0	2.9				
				153						87.6	1.6	2.49	71.4	2.91	10.0	3.9	2.8				
				170	tr	7	38	55	7.9	77.2	1.60	2.14	68.2	2.84	15.7	4.2	3.7	67	43	24	1.43
				190						81.6	1.58	2.24	69.1	2.81	11.4	3.2	3.6				
				210						66.7	1.56	1.86	65.0	2.85	11.1	4.0	2.8				
				213	0	21	35	44	6.13									51	30	21	
				221						55.7	1.74	1.56	60.9	2.86	9.0*	5.2*	1.8				

Table 1 continued

Station	Latitude	Water depth (m)	Depth in core (cm)	Grain size (weight percent)				Mean grain size $\phi$	Water content (%)	Wet bulk density (gm/cm <sup>3</sup> )	Void ratio	Porosity (%)	Grain specific gravity	Vane shear strength (kPa)			Atterberg limits				
				coarse	sand	silt	clay	undisturbed						remolded	sensitive	liquid limit (%)	plastic limit (%)	plasticity index (%)	liquid-ity index		
509	57°21.19'N 155°08.66'W	225	0	0	tr	34	66	8.6													
			5	0	1	42	57	8.2										83	45	38	
			12	0	1	45	54	8.1	123.8	1.42	3.34	77.0	2.76	3.5	0.9	3.9					
			30						111.8	1.46	3.06	75.4	2.80	4.9	1.8	2.7					
			48						121.3	1.44	3.33	76.9	2.81	4.1	2.5	1.7					
			70						120.6	1.44	3.35	77.0	2.84	4.0	1.6	2.4					
			90	0	2	43	55	8.1	113.5	1.45	3.05	75.3	2.75	4.9	1.6	3.0	46	26	20	4.73	
			111						115.3	1.46	3.18	76.1	2.83	4.9	1.6	3.0					
			132	0	1	40	59	8.3	104.7	1.49	2.92	14.5	2.85	7.2	1.7	4.2	85	45	40	1.49	
			152						100.6	1.51	2.82	73.8	2.87	10.8	3.4	3.2					
			172	0	1	42	57	8.2	96.6	1.51	2.68	72.9	2.84	11.5	3.5	3.3	78	45	33	1.56	
			192						94.8	1.52	2.62	72.4	2.83	10.0	3.3	3.0					
			212	0	tr	38	62	8.5	98.2	1.49	2.74	73.3	2.77	8.5	2.6	3.3	82	41	41	1.40	
510	57°39.22'N 155°17.18'W	305	0	0	2	41	57	8.2													
			15	0	3	48	49	7.8	119.2	1.44	3.23	76.4	2.77	4.0*	2.2*	1.8					
			30	0	2	48	50	7.9	107.7	1.47	2.89	74.3	2.74	3.1	1.2	2.7	70	34	36	2.05	
			37	0	4	54	42	7.3									69	41	28		
			50						89.7	1.51	2.30	69.7	2.62	5.8	1.4	4.2					
			70						101.0	1.50	2.81	73.9	2.86	5.7	1.9	3.0					
			90	0	2	45	53	8.0	96.4	1.51	2.62	72.4	2.78	4.9	1.8	2.1	69	42	27	2.01	
			107	0	2	45	53	8.0	98.8	1.51	2.75	73.3	2.84	7.9	2.2	3.6					
			115						87.9	1.55	2.45	71.0	2.85	5.0*	2.0*	2.5					
			125						88.8	1.55	2.46	71.1	2.83	9.3	3.3	2.8					
			145	0	2	46	52	8.0	96.5	1.44	3.48	77.7	2.89	7.2	2.2	3.2	74	41	33	1.68	
			165						87.3	1.56	2.46	71.1	2.88	8.8	4.8	1.8					
			185	0	3	48	49	7.8	87.3	1.55	2.41	70.6	2.82	9.4	3.5	2.7					
200	0	3	46	51	7.9									69	36	33					
205						68.5	1.63	1.81	64.8	2.75	15.5	4.4	3.5								
215						81.9	1.57	2.22	68.9	2.77	7.8*	3.6*	2.1								

Table 1 continued

Station	Latitude	Longitude	Water depth (m)	Core (cm)	Grain size (weight percent)			Mean grain size $\phi$	Water content (%)	Wet bulk			Grain Vane shear strength (k Pa)			Atterberg limits					
					coarse sand	silt	clay			density ( $\text{gm/cm}^3$ )	Void ratio	Porosity (%)	specific gravity	undisturbed	sensitized	remolded	liquid limit (%)	plastic limit (%)	plasticity index (%)	liquid-plasticity index	
511	57°39.08'N	154°50.14'W	214	0	0	1	33	66	8.6												
				15	0	1	44	55	8.2	109.5	1.45	2.89	74.3	2.88	2.6	1.4	1.9	74	38	36	1.99
				35						113.8	1.48	3.11	75.7	2.89	3.3	1.7	1.9				
				65						105.7	1.47	2.82	73.8	7.73	4.5	1.6	2.8				
				85	0	1	46	53	8.1	103.1	1.48	2.73	73.2	7.71	6.2	2.1	3.0				
				93	0	1	46	53	8.1									76	42	34	
				105						101.2	1.51	2.87	74.2	2.90	6.8	2.8	2.4				
				125						99.5	1.52	2.83	73.9	2.91	9.7	3.1	3.1				
				145	0	1	45	54	8.1	91.9	1.55	2.62	72.4	2.92	9.4	3.4	2.8	69	21	48	1.48
				165						95.1	1.52	2.64	72.5	2.84	9.9	3.3	3.0				
				190						86.2	1.54	2.28	69.5	7.70	10.6	3.4	3.1				
				210	0	1	44	55	8.2	84.7	1.57	2.38	70.5	2.88	13.5	4.9	2.7	70	44	26	1.57
				230						86.9	1.56	2.41	70.7	2.84	11.9	4.8	2.5				
512	57°52.5' N	154°14.9' W	195	0	0	1	40	20	6.8												
				13	0	1	52	48	7.9	103.9	1.46	2.65	72.6	2.81	6.2	1.4	4.4	71	41	30	2.04
513	57°54.8' N	154°19.8' W	205	0	0	2	46	52	8.0												
				12	0	1	43	54	8.0	96.2	1.51	2.61	72.3	2.77	3.2	1.2	2.8	67	37	30	1.97
514	57°55.3' N	154°25.0' W	222	0	0	3	51	46	7.7												
				27	0	1	5	57	43	7.5								63	36	27	
				28	0	1	4	52	44	7.6	89.7	1.55	2.50	71.4	2.85	4.0	1.0	2.4			
515	57°59.0' N	154°27.3' W	238	0	1	4	62	33	7.1												
				74						61.5	1.65	1.59	61.4	2.7	6.5	5.0	1.4	2.1			
516	58°00.3' N	154°10.6' W	205	0	0	3	56	41	7.5												
				10						87.1	1.52	2.26	69.3	2.65	3.6	2.6	1.4				

Table 1 continued

Station	Latitude	Water depth (m)	Depth in core (cm)	Grain size (weight percent)				Mean grain size $\phi$	Water content (%)	Wet bulk			Grain specific gravity	Vane shear strength (kPa)			Atterberg limits			
				coarse	sand	silt	clay	size		density (gm/cm <sup>3</sup> )	Void ratio	Porosity (%)		undisturbed	remolded	sensitivity	liquid limit (%)	plastic limit (%)	plasticity index (%)	liquid-ity index
517	57°55.3'N	180	0	0	1	38	61	8.4												
	154°00.9'W		15	0	1	52	47	7.8	111.5	1.46	3.04	75.2	2.78	4.9	1.2	8.2	72	39	33	2.20
518	58°00.3'N	180	0	0	1	37	62	8.4												
	153°51.6'W		15	0	2	49	48	7.8	103.8	1.47	2.71	73.1	2.67	5.4	1.8	3.0				
			28						87.3	1.51	2.18	68.8	2.56	4.0	1.3	3.0				
519	58°05.5'N	200	0	0	3	46	51	7.9												
	154°01.3'W		15	0	6	52	42	7.4	114.2	1.44	3.01	75.0	2.69	4.1	0.7	5.6	65	39	26	2.89
520	58°13.2'N	213	0	0	6	46	48	7.6												
	153°56.2'W		9												3.4	0.7	4.6			
			12						115.4											
			15	0	9	52	39	7.2	95.1	1.50	2.51	71.5	2.70	3.2	0.2	19.5	5P	34	24	2.55
			27												2.9	0.6	5.0			
			27												4.0	1.2	4.2			
35						89.2	1.54	2.40	70.6	2.76					57	34	23	2.40		
38						71.0	1.61	1.87	63.1	2.69	6.0*	3.2*	1.9							
521	58°07.93'N	179	0	0	1	40	59	8.3												
	153°45.93'W		12	0	4	49	47	7.7												
522	58°05.5'N	185	0	0	1	37	62	8.4												
	153°41.4'W		6	0	2	49	49	7.9	126.4	1.40	3.21	76.3	2.60	3.1	1.6	1.9	86	45	41	1.99
523	58°01.7'N	130	0					44.3	1.82	1.20	54.8	2.78	9.8*	1.6*	6.0					
	153°34.2'W		10					40.7	1.87	1.17	52.8	2.81	10.2*	1.4*	7.8					
			210					44.1	1.81	1.71	54.7	2.80	10.8*	3.2*	3.3					
			276					43.6	1.85	1.22	55.0	2.87	9.8*	2.6*	3.7					

103 100ed

Station	Latitude	Longitude	Water depth (m)	Depth in core (cm)	Grain size (weight percent)				Water content (%)	Wet bulk density (gm/cm <sup>3</sup> )	Void ratio	Porosity (%)	Grain specific gravity	Vane shear strength (kPa)			Atterberg limits				
					coarse	sand	silt	clay						undisturbed	sensitized	remolded	liquid limit (%)	plastic limit (%)	plasticity index (%)	liquid-plasticity index	
524	58°15.94'N	153°41.87'W	175	11	14	51	35	6.8													
525	58°23.7'N	153.37 .2, w	158	0	43	31	27	5.2													
				15					45.7	1.80	1.24	55.3	2.77	9.5	1.6	5.8					
				35					45.0	1.82	1.23	55.2	2.80	23.5	5.4	4.4					
				55	0	33	42	25	43.8	1.82	1.19	54.2	2.77	31.3	5.6	5.6	40	233	12	1.32	
				85					40.5	1.86	1.10	52.3	2.77	27.33	6.6	4.2					
				100					53.9	1.77	1.38	58.0	2.79	17.1	3.3	5.2					
				125	0	22	44	34	6.4	56.3	1.73	1.56	60.9	2.83	11.5	3.2	3.6	43	27	16	1.133
				145					43.0	1.75	1.18	54.2	2.82	20.2	3.9	5.2					
				165	0	60	21	19	4.0	35.1	1.92	0.95	48.8	2.78	35.7	8.3	4.3	35	25	10	1.01
526	58°29.0'N	153°27.1'W	138	0	48	31	21	4.7													
				20					49.6	1.78	1.36	57.6	2.80	7.1	2.0	3.6					
				40					46.4	1.80	1.27	55.9	2.79	11.5	3.3	3.5					
				65	0	30	45	25	5.6	45.3	1.81	1.23	55.1	2.77	7.6	2.3	3.3				
				77										8.0*	2.6*	3.0					
				85					38.6	1.85	1.08	51.9	2.75	11.7	2.6	4.1					
				100					47.4	1.83	1.23	55.1	2.81	14.8	3.3	4.4					
				125	0	33	41	26	5.6	51.1	1.80	1.29	56.3	2.80	10.1	1.7	3.4				
				129	0	75	43	32	6.1								43	27	16		
				145					49.1	1.72	1.55	60.7	2.80	18.5	4.0	3.13					
				165					41.7	1.81	1.28	56.1	2.82	11.0	3.0	3.7					
				171	0	33	49	28	5.6								35	23	12		

Table 1 continued

Station	Latitude	Longitude	Water depth (m)	Depth in core (cm)	Grain size (weight percent)				Mean grain size $\phi$	Water content (%)	Wet bulk			Grain Vane shear strength (kPa)				Atterberg limits				
					coarse	sand	silt	clay			density (gm/cm <sup>3</sup> )	Void ratio	Porosity (%)	specific gravity	undisturbed	remolded	sensitivity	liquid limit (%)	plastic limit (%)	plasticity index (%)	liquid-liquidity index	
527	58°34.2'N 153°17.6'W		153	0	0	56	23	21	4.3													
				15**	11	42	30	17	3.9	36.8	1.90	1.00	50.0	7.7R	16.4	4.9	3.4	34	22	12	1.23	
				23						37.7	1.88	1.01	50.2	7.74	13.0*	1.8*	7.2					
				35						33.1	1.95	0.90	47.3	2.77	19.4	4.9	-3.9					
				55						32.4	1.94	0.87	46.4	2.74	8.6	2.1	4.2					
				58						34.4	1.92	0.92	48.0	2.74								
				70**	11	69	11	9	2.4	31.5	1.95	0.84	45.6	2.73	15.2	3.3	4.6	20				
				95						38.0	1.89	1.03	50.8	2.79	26.7	6.6	4.1					
528	58°39.4'N 153°0.7'W		159	115**	13	50	20	17	3.3	36.3	1.86	0.94	48.4	2.65	16.1	3.7	4.3	29	23	6	2.72	
				123						23.3	2.07	0.62	38.3	2.72	19.8*	3.2*	6.0					
				0	8	33	30	29	5.0													
				15	1	37	38	24	5.2	40.6	1.84	1.08	52.0	2.73	21.7	4.2	5.2	35	23	12	1.47	
528	58°39.4'N 153°0.7'W		159	35						53.5	1.73	1.44	59.0	2.75	15.6							
				52						47.8	1.79	1.30	56.5	2.78	11.6*	2.8*	4.2					
				62						43.8	1.84	1.20	54.8	2.81	16.6	5.0	3.3					
				82	tr	43	30	27	5.2	49.0	1.75	1.28	56.2	2.68	11.4	1.6	7.0	38	26	12	1.92	
				94						38.2	1.87	1.01	50.4	2.72	15.6	3.1	5.0					
				119						44.2	1.80	1.17	54.0	2.71	22.2	6.6	3.4					
				146	tr	30	35	35	6.0	54.0	1.72	1.43	58.9	2.71	15.7	5.7	2.8	30	24	15	2.00	
				152						46.6	1.78	1.23	55.1	2.70	17.0*	5.8*	2.9					
				175						47.1	1.78	1.25	55.6	2.72	17.2	1.5	3.8					
				190						51.5	1.71	1.43	58.0	2.74	16.3	3.0	4.2					
				210	3	16	30	31	5.4	52.0	1.73	1.38	57.9	2.71	16.6	4.5	3.7	36	31	5	4.20	
214						47.8	1.79	1.31	56.7	2.80	15.6	4.0	3.0									
222						48.4	1.80	1.14	57.2	2.83	16.2*	1.6*	3.8									

Table 1 continued

Station	Latitude	Longitude	Water depth (m)	Core no.	Grain size (weight percent)				Mean grain size	Water content (%)	Wet bulk			Grain Vane shear strength (kPa)			Atterberg limits					
					coarse	sand	silt	clay			density (gm/cm <sup>3</sup> )	Void ratio	Porosity (%)	specific gravity	undisturbed	sensitively remolded	liquid limit (%)	plastic limit (%)	plasticity index (%)	liquid-plasticity index		
529	58°44.4'N 152°57.4'W	136			0	0	39	29	32	5.5												
					15	0	27	41	32	6.1		1.85	1.01	30.3	2.68							
					55	4	71	16	9	2.8		1.85	1.01	50.3	2.68							
					60						38.4						11.6*	3.4*	3.4			
					110						27.9	1.99	0.74	42.5	2.71	14.2*	4.0*	3.6				
					200								19.6*	3.2*	6.3							
530	58°49.7'N 152°47.6'W	165			0	1	76	10	13	3.0												
					15	tr	68	16	16	3.6	41.1	1.83	1.08	52.0	2.70	12.4	3.1	3.9				
					35	tr	77	11	12	3.0	42.3	1.79	1.09	52.1	2.63	10.2	1.3	7.8				
					40												4.2*					
					47							1.75	1.26	55.7	2.67	4.2*						
531	58°54.9'N 152°37.3'W	161			0	4	87	3	6	2.0												
											41.9						16.2	3.1	5.2			
532	58°45.85'N 152°27.98'W	195			0	54	44	tr	2	-0.2												
533	58°50.4'N 152°23.9'W	120			0	100	0	0	0	-2.0												
					15												6.0	2.1	2.9			
533	58°39.6'N 152°47.1'W	185			0	0	37	41	22	5.2												
					15	0	47	24	29	5.0	49.7	1.76	1.33	57.2	2.75	19.6	3.5	5.5	44	29	15	1.38
					35						41.0	1.83	1.08	51.9	2.69	19.1	4.2	4.5				
					49	0	68	15	17	3.6										38	32	6
					60	tr	60	18	22	4.2	45.6						30.1	7.2	4.2	41	30	11
					83								58.1	1.65	1.44	59.0	2.54	23.8*	2.4*	10.4		

Table continued

Station	Latitude	Longitude	Water depth (m)	Depth in core (cm)	Grain size (weight percent)				Mean grain size	Water content (%)	Wet bulk		Porosity (%)	Grain specific gravity	Vane shear strength (kPa)			Atterberg limits			
					coarse	sand	silt	clay	φ		density (gm/cm <sup>3</sup> )	Void ratio			undisturbed	remolded	sensitivity	liquid limit (%)	plastic limit (%)	plasticity index (%)	liquid-ity index
535	19°37.0'N		98	0	5	89	2	4	1.8												
	112°42.0'W			15	0	0	56	44	7.8	39.4	1.51	2.61	72.3	2.76	14.2	1.8	7.9				
	19°44'N		190	0	0	17	35	48	7.2												
	112°6'W			15	u	13	44	43	7.1	77.5	1.57	2.02	66.8	2.66	11.3	2.3	4.9	68	43	25	1.38
				30						82.9	1.58	2.33	70.0	2.88							
				35											9.7	2.8	3.5				
				40						76.5	1.59	2.06	67.3	2.75	7.4*	2.4*	3.0				
				55						77.1	1.60	2.13	68.0	2.82	9.9	2.1	4.8				
				75						66.2					10.4	2.6	3.9				
				91	1	35	27	37	5.8	69.7	1.63	1.88	65.3	2.76	7.1	2.2	3.2	48	31	17	2.28
				111						49.2	1.76	1.31	56.0	2.73	13.9	3.2	4.3				
				129						43.9	1.83	1.21	54.7	2.81	10.6	2.1	5.2				
				14(1						39.0	1.87	1.07	51.6	2.78	6.0*	2.6*	2.3				
				150						41.5	1.86	1.15	53.4	2.81	16.4	4.9	3.3				
				170	0	11	45	44	7.3	44.2					11.9	3.0	3.9	37	23	14	1.51
				190						48.6					4.5	1.6	2.8				
				210						48.2					9.0	2.9	3.1				
				240						51.3					11.6*	3.2*	3.6				

Table 1 continued

Station	Latitude	Longitude	Water depth (m)	Depth in core (cm)	Grain size (weight percent)			Mean grain size	Water content (%)	Wet bulk		Porosity (%)	Grain Vane shear strength (k Pa)			Atterberg limits					
					coarse sand	silt	clay	φ		density (gm/cm <sup>3</sup> )	Void ratio		undisturbed	sensitized	remolded	liquid limit (%)	plastic limit (0)	plasticity index (9)	liquid-plasticity index		
537	58°29.0'N	160	0	0	23	36	41	6.6													
			153°07.6'W	20	0	14	44	43	7.2	67.6	1.66	1.88	65.2	2.84	9.0	2.6	3.4	57	34	23	1.46
				40					64.5	1.67	1.71	63.9	2.81	15.8	4.7	3.4					
				60					63.5	1.67	1.74	63.5	2.80	17.6	4.8	3.7					
				75	0	18	38	45	7.0					17.1	4.7	3.6	56	30	26		
				85					64.7	1.67	1.77	63.9	2.80	14.6*	3.2*	4.5					
				100					59.4	1.69	1.61	61.6	2.77	27.0	6.8	4.0					
				120					71.2	1.63	1.97	66.3	2.83	27.8	7.5	3.7					
				139	0	37	32	31	5.6	55.1	1.72	1.48	59.7	2.75	22.2	5.5	4.0				
				157					53.8	1.73	1.45	59.1	2.75	22.1	6.1	3.6					
				176					53.5	1.74	1.44	59.1	2.76	25.4	6.3	4.0					
				185					54.7	1.72	1.46	59.3	2.73	18.2*	4.2*	4.4					
	538	38°25.2'N	190	0	0	18	35	47	7.1												
153°00.2'W				15	0	46	24	30	5.1	87.9	1.54	2.44	70.9	2.79	7.3	2.1	3.6	70	32	38	1.47
				24					88.9	1.54	2.41	70.7	2.77	13.2*	3.2*	4.0					
				35					86.9	1.55	2.36	70.3	2.78	9.9	3.3	3.0					
				55					79.2	1.58	2.15	68.2	2.77	13.9	3.4	4.1					
				75	0	7	42	51	7.7	86.4	1.55	2.36	70.2	2.79	9.1	2.4	3.8	70	41	29	1.57
				95					79.8	1.59	2.20	68.8	2.82	14.9	4.0	3.7					
				115					63.2	1.69	1.77	64.0	2.87	25.9	6.7	3.9					
				124					63.1	1.67	1.71	63.1	2.77	23.0*	5.8*	4.0					
				135	u	18	38	44	7.0	70.2	1.62	1.89	65.4	2.75	15.8	4.2	3.8	60	31	29	1.35
				155					55.0	1.73	1.49	59.9	2.78	29.2	8.9	3.3					
				175					68.4	1.56	2.33	69.9	2.82	22.2	5.9	3.7					
				195	0	26	38	35	6.2	55.9	1.72	1.51	60.2	2.77	24.6	5.0	4.4	48	29	19	1.42
			205					65.1	1.66	1.77	63.9	2.78	17.0	6.4	2.6						
			224					61.1	1.69	1.65	62.2	2.79	16.4*	5.8*	2.9						

Tabl - 1 continued

Station	Latitude	Water depth (m)	Depth in core (m)	Grainsize (weight percent)				Mean grain size	Water content (%)	Wet bulk			Grain Vane shear strength (kPa)				Atterberg limits			
				coarse	sand	silt	clay	φ		density (gm/cm <sup>3</sup> )	Void ratio	Porosity (%)	specific gravity	undisturbed	remolded	sensitivity	liquid limit (%)	plastic limit (%)	plasticity index (%)	liquid-ity index
539	58°21.3'N 153°12.4'W	175	0	n	9	36	55	7.8												
			15	o	4	47	49	7.8												
			60						89.7	1.54	2.47	71.2	2.82	9.8*	3.2*	3.1				
			65	o	3	42	55	8.1												
			110						150.8	1.37	4.1R	HO. ?	2.83	7.2*	4.0*	3.3				
			135				89.5	1.54	2.46	71.1	2.81	10.2*	3.2*	3.1						
540	58°21.5'N 153°07.6'W	210	0	o	20	45	35	6.5												
			15	o	20	35	45	6.9												
			60						76.9	1.58	2.07	66.8	2.68	13.6*	2.8*	4.8				
			110						79.2	1.58	2.15	68.3	2.78	14.6*	4.0*	3.7				
			204						51.6	1.75	1.40	58.3	2.77	27.0*	6.2*	4.3				
			248				48.2	1.79	1.32	56.9	2.80	23.8*	5.0*	4.8						
541	58°15.8'N 153°22.0'W	167	0	o	4	41	55	8.0												
			15	n	5	57	37	7.2	96.1					5.0	1.6	3.2	63	39	24	2.30
542	58°18.6'N 153°26.9'W	155	0	o	9	47	44	7.4												
			15	o	15	55	30	6.5	76.7					5.9	2.0	3.0	56	35	21	1.99
543	58°10.77'N 153°11.37'W	180	0	o	2	48	50	7.9												

37



Table 1 continued

Station	Latitude	Longitude	Water depth (m)	Depth in core (cm)	Grain size (weight percent)				Mean grain size	Water content (%)	Wet bulk			Grain Vane shear strength (k Pa)				Atterberg limits				
					coarse	sand	silt	clay	φ		density (gm/cm <sup>3</sup> )	Void ratio	Porosity (%)	specific gravity	undisturbed	sensitized	remolded	liquid limit (%)	plastic limit (%)	plasticity index (%)	liquid-ity index	
548	58°37.9'N 153°25.1'W		64	0	tr	7	57	3A	7.1													
				20	o	0	67	34	7.4	54.2	1.72	1.44	59.0	2.72	4.9	1.6	3.0	40	19	21	106L3	
				40						53.7	1.72	1.42	58.6	2.70	6.3	1.6	3.8					
				60	o	7	62	11	6.9	60.7	1.68	1.63	62.0	2.75	4.9	0.9	5.5	30	29	1	26.0	
				80						50.7	1.75	1.35	57	5	2.73	6.4	2.3	2.8				
			90					56.1	1.70	1.47	59.5	2.68	5.6	1.6	3.4							
549	58°43.3'N 153°15.0'W		87	0	2	30	28	40	6.1													
				15	o	26	53	21	5.7	43.6	1.82	1.14	53.2	2.73	9.4	1.7	5.4	29	25	4	4.65	
				30						45.4	1.78	1.18	54.2	2.67	12.3	2.1	6.0					
				42						51.1	1.74	1.34	57.3	2.89	5.2*	2.0*	2.7					
550	58°50.8'N 153°10.3'W		165	0**	9	63	14	14	3.0													
				15**	o	41	37	22	5.0	42.4	1.79	1.09	52.0	2.62	37.5	5.4	7.0	30				
				35						41.2	1.84	1.10	57.5	2.74	11.9	3.3	3.6					
				55						37.8	1.89	1.03	50.7	2.78	22.2	1.6	8.4					
				84	2	52	28	13	4.3	39.3	1.85	1.04	51.1	2.77	27.9	2.7	10.3	28	21	7	2.61	
				100						41.7	1.83	1.11	52.6	2.72	15.6*	2.0*	7.9					
				124						39.1	1.86	1.04	51.1	2.72	20.2	3.3	6.7					
				144**	o	51	29	20	4.5	14.2	1.92	0.93	47.7	2.73	16.1	1.5	10.8	26				
				158						30.8	1.98	0.83	45.5	2.17	18.0	2.6	7.2					
175						11.4	1.94	0.86	46.3	2.72	11.4*	1.4*	8.6									
551	58°53.6'N 152°04.4'W		155	0	o	32	36	32	5.8													
				15	o	28	43	29	5.9	56.1	1.72	1.51	60.1	2.79	10.6	2.1	5.2	43	26	17	1.77	
				35						44.8	1.81	1.31	54.7	2.76	18.8	2.7	6.6					
				55	o	55	27	18	4.2	37.8	1.89	1.02	50.5	2.77	22.6	4.0	5.6	29	25	4	3.20	
			75					30.2	1.97	0.80	44.5	2.72	20.2*	4.0*	5.1							



Table 2. Replicate vane shear measurements on split-core halves.  $S_u$  indicates undisturbed strength,  $S_r$  indicates remolded strength, subscript 1 refers to first core half, subscript 2 refers to second.  $V_u$  and  $V_r$  are the coefficients of variation for replicate undisturbed and remolded strength measurements, respectively. The notation **tc-sp** indicates that a torque cell was used to measure strength on the first core half and a spring was used on the second, whereas **tc-tc** indicates that torque-cell measurements were made on both halves.

<u>Core</u>	<u>Depth in core (cm)</u>	$S_{U1}$ <u>(kPa)</u>	$S_{U2}$ <u>(kPa)</u>	$S_{r1}$ <u>(kPa)</u>	$S_{r2}$ <u>(kPa)</u>	$V_u$ (%)	$V_r$ (%)
508 G1	13	3*1	3.5	0.8	1.3	12	48
(tc-tc)	35	4.9	3.2	0.9	1.2	42	29
	55	8.2	9.5	2.1	2.5	15	17
	75	9.0	7.3	2.6	1.8	21	36
	110	9.0	10.0	2.6	2.6	11	0
	130	11.6	14.8	4.0	4.7	24	16
	153	10.8	12.4	3.5	3*5	14	0
	170	15.7	14.3	4.2	3*9	9	7
	190	11.4	15.6	3.2	4.1	31	25
	210	11.1	21.6	4.0	2.6	64	42
511 G1	15	2.6	3.22	1.4	1.6	21	13
(tc-sp)	65	4.5	6.0	1.6	2.4	29	40
	85	6.2	5.2	2.1	2.5	18	17
	105	6.8	7.5	2.8	3.3	10	16
	125	9.7	7.8	3.1	3.0	22	3
	145	9.4	7.8	3.4	3.6	19	6
	165	9.9	7.8	3.3	3*3	24	0
	190	10.6	11.3	3.4	4.6	6	30
	210	13.5	13.2	4.9	5*9	2	19
	230	11.9	10.2	4.8	4.8	15	0

<u>Core</u>	<u>Depth in core (cm)</u>	<u>s<sub>u1</sub></u> (kPa)	<u>s<sub>U2</sub></u> (kPa)	<u>s<sub>r1</sub></u> (kPa)	<u>s<sub>r2</sub></u> (kPa)	<u>v<sub>u</sub></u> (%)	<u>v<sub>r</sub></u> (%)
525 G1	15	9.5	9.5	1.6	2.6	0	48
(tc-tc)	35	23.5	10.5	5.4	3*7	76	37
	55	31.3	19.04	5.6	5*1	47	9
	85	27.8	24.0	6.6	6.5	15	2
	105	17.1	17*4	3.3	4.9	2	19
	125	11.5	11.4	3.2	4*0	1	22
	145	20.2	17.4	3.9	4.0	15	3
	165	35*7	28.1	8.3	7.5	24	10
526 G2	20	7.1	<b>7.5</b>	2.0	2.3	5	<b>14</b>
(tc-sp)	40	11.5	7*9	3.3	2.3	37	36
	65	7.6	9.3	2.3	2.5	20	8
	85	10.7	6.6	2.6	2*2	47	17
	105	14.3	13.8	3.3	4.5	4	31
	125	5*9	8.3	1.7	2.2	34	26
	145	18.5	14.4	4.9	4.9	25	0
	165	<b>11.0</b>	4.9	3.0	2*2	77	31

<u>Core</u>	Depth in core (cm)	$s_{u1}$ (kPa)	$s_{u2}$ (kPa)	$s_{r1}$ (kPa)	$s_{r2}$ (kPa)	$V_u$ (%)	$V_r$ (%)
528 G3	15	21.7	27.1	4.2	15.0	22	113
(tc-sp )	62	16.6	16.0	5.0	4*4	4	13
	82	11.4	19.1	1.6	4*1	50	88
	94	15.6	15.7	3.1	6.4	1	69
	119	22.2	19.3	6.6	6*6	14	0
	146	15.7	19.5	5.7	7.6	22	29
	175	17.2	20.8	<b>4.5</b>	6.8	19	41
	190	16.3	20.2	3.9	5.4	21	32
	210	16.6	13.4	4.5	3*9	<b>21</b>	14
	234	1506	18.2	4.0	5.4	15	30
545 G1	50	9.3	6.2	2.2	1.6	40	32
(tc-tc)	70	6.6	5.4	2.2	2.1	20	5
	90	5.6	4.5	1.7	1.5	22	12
	<b>106</b>	11.4	5.3	2.6	1.0	73	89
	130	13.3	15.2	3.3	<b>4.1</b>	13	22
	150	11.4	9.6	5.1	3.3	17	5
	170	11.4	17.6	4*0	5.4	43	30
	185	11.1	9.4	3.8	3.4	17	11
	205	11.0	13.8	<b>3.1</b>	3.3	23	6
	225	12.3	10.0	<b>3.1</b>	3.8	21	21
	245	11.6	13.2	2.3	<b>5.4</b>	13	<b>81</b>
	265	14.2	14.0	4.0	5.6	1	33

Table 3. Strength anisotropy in sediment cores.  $S_{ue}$  is the undisturbed vane shear strength measurement taken on ends of core sections, and  $S_{us}$  is the corresponding predicted split-core value.  $S_{re}$  and  $S_{rs}$  are the measured and predicted remolded vane shear measurements, respectively. Corrected  $S_{ue}$  =  $S_{ue} - (S_{re} - S_{rs})$ . (Negative strength values are an artifact of the analytical procedure. These values are not used in Fig. 113)

44

Core	Depth in core (cm)	Water content (%)	Estimated plasticity index (%)	$S_{ue}$ (kPa)	Corrected $S_{ue}$ (kPa)	$S_{us}$ (kPa)	$S_{re}$ (kPa)	$S_{rs}$ (kPa)	Anisotropy
508	21	106.2	42	5.0	3.4	4.4	2.6	1.0	1.3
	121	66.4	31	4.2	7.2	15.1	2.0	5.0	2.1
	221	55.7	21	9.0	9.9	17.9	5.2	6.1	1.8
510	15	119.2	36	4.0	2.0	-0.1	2.2	0.2	-0.1
	<b>115</b>	87.9	27	5.0	6.0	9.0	2.0	3.0	<b>1.5</b>
527	23	37.7	12	13.0	16.8	22.0	1.8	5.6	1.3
	123	23.3	6	19.8	15.2	-4*4	3.2	-1.4	-0.3
528	52	47.8	12	11.6	13.0	16.8	2.8	4.2	1*3
	152	46.6	15	17.0	15.4	17.0	5.8	4.2	1.1
534	83	58.1	<b>11</b>	23.8	25.5	24.3	2.4	4.1	1.0
536	40	76.5	25	7.4	7.1	9.3	2.4	2.1	1.3
	140	39.0	<b>14</b>	6.0	6.6	<b>11.6</b>	2.6	3.2	1.8
	240	51.3	14	11.6	11.2	10*9	3.2	2.8	1.0
537	85	64.7	23	14.6	16.8	19.8	3.2	5.4	1.2
	185	54.7	23	18.2	19.9	22.8	<b>4.2</b>	5.9	1.2
538	24	88.9	38	13.2	12.3	8.0	3.2	2.3	0.6
	124	63.1	29	23.0	23.4	22.6	5.8	6.2	1.0
	224	61.1	19	16.4	17.1	23.7	5.8	6.5	1.4
545	97	65.3	26	8.8	9.8	11.0	2.0	3.0	<b>1.1</b>
	184	55.6	17	<b>14.4</b>	12.8	<b>12.8</b>	5.0	3.4	1.0

Table 3 cont.

Core	Depth in core (cm)	Water content (%)	Estimated plasticity index (%)	S <sub>ue</sub> (kPa)	Corrected S <sub>ue</sub> (kPa)	S <sub>us</sub> (kPa)	S <sub>re</sub> (kPa)	S <sub>rs</sub> (kPa)	Anisotropy
547	27	62.8	13	5.0	4.4	4.9	1.8	1.2	1.1
	67	57.4	14	6.6	6.2	6.5	2.0	1.6	1.0
550	100	41.7	7	15.6	16.7	19.7	2.0	3.1	1.2
	175	31.4	7	11.4	12.5	20.9	1.4	2.5	1.7
551	75	30.2	4	20.2	20.7	27.6	4.0	4.5	1.3
552	69	47*5	14	12.2	13.0	15.5	2.6	3.4	1.2
	89	46.1	14	29.4	26.5	16.4	6.6	3.7	0.6
	<b>174</b>	41.5	18	19.2	19.6	19.5	4.2	4.6	1.0

Table 4. Clay mineralogy of tops of cores.

Station	% chlorite	% illite	% mixed layer	% smectite in mixed layer	Corrected % smectite	Corrected % illite
507	42	<b>53</b>	<b>5</b>	75	4	54
508	43	<b>49</b>	<b>8</b>	75	6	51
509	44	<b>47</b>	<b>9</b>	75	7	49
510	44	56	<b>0</b>	0	0	56
511	41	51	<b>8</b>	<b>75</b>	6	53
512	44	47	<b>9</b>	81	7	49
513	40	52	<b>8</b>	75	6	54
514	42	53	<b>5</b>	70	4	54
515	40	53	<b>7</b>	80	6	54
516	37	58	<b>5</b>	75	4	59
517	46	46	<b>8</b>	80	6	48
518	40	52	<b>8</b>	70	6	54
519	47	47	<b>6</b>	75	5	48
520	46	50	<b>4</b>	79	3	51
521	39	52	<b>9</b>	75	7	54
522	43	50	<b>7</b>	70	5	52
523	40	52	<b>8</b>	74	6	54
525	38	56	<b>6</b>	75	5	57
526	45	48	<b>7</b>	79	6	<b>49</b>
527	37	56	<b>7</b>	79	6	57
528	37	56	<b>7</b>	75	5	58
529	34	54	<b>12</b>	75	9	57
530	40	47	<b>13</b>	79	<b>10</b>	50
531	51	42	<b>7</b>	75	5	<b>44</b>
532	40	41	<b>19</b>	70	13	47
534	46	48	<b>6</b>	75	5	49
535	42	29	<b>29</b>	77	22	36
536	47	46	<b>7</b>	76	5	48
537	42	49	<b>9</b>	77	7	51
538	44	50	<b>6</b>	80	5	51
539	43	48	<b>9</b>	81	7	50
540	49	44	<b>7</b>	80	6	45
541	47	47	<b>6</b>	77	5	48
542	47	47	<b>6</b>	84	5	48
543	45	44	<b>11</b>	70	8	<b>47</b>
545	44	48	<b>8</b>	77	6	50
546	45	48	<b>7</b>	75	5	50
547	48	46	<b>6</b>	75	5	<b>47</b>
548	32	60	<b>8</b>	79	6	62
549	40	54	<b>6</b>	75	5	55
550	38	56	<b>6</b>	<b>79</b>	5	57
551	45	50	<b>5</b>	75	4	51
552	35	58	<b>7</b>	82	6	59
553	37	53	<b>10</b>	91	9	54

Table 5. Clay mineralogy (percents) of Shelikof Strait and possible source areas.

	<u>Shelikof Strait</u>		<u>Cook Inlet</u>		<u>Kodiak Shelf</u>		<u>Copper River and Delta</u>	
	<u>average</u>	<u>range</u>	<u>average</u>	<u>range</u>	<u>average</u>	<u>range</u>	<u>average</u>	<u>range</u>
chlorite	42	32-51	42	29-64	51	30-69	56	53-64
illite	52	36-66	46	32-61	34	19-43	31	27-39
smectite	6	0-22	3	0-19	5	0-30	tr	o-1

Table 6. Light hydrocarbon gas contents of sediment cores.

Station	Depth in core (cm)	C <sub>1</sub>	C <sub>2</sub>	C <sub>2</sub> :I	C <sub>3</sub>	i-C <sub>4</sub>	n-C <sub>4</sub>	C <sub>1</sub>	C <sub>2</sub>
		Methane (μl/l)	Ethane (nl/l)	Ethene (nl/l)	Propane (nl/l)	Isobutane (nl/l)	n-butane (nl/l)	C <sub>2</sub> +C <sub>3</sub>	C <sub>2</sub> . 1 <sup>-</sup>
509	100-110	177	228	248	224	24	42	390	0.9
511	96-106	36	46	12	52	0	0	365	3.9
514	30-40	23	48	28	46	14	0	247	1.7
523	100-110	10	24	22	44	0	0	156	1*I
525	100-110	1	0	0	0	0	0		
526	50-60	18	116	100	116	26	14	80	1.2
	700-110	16	36	28	80	18	0	<b>137</b>	<b>1.3</b>
	200-210	38			66				
527	100-110	25	202	300	192	26	24	62	0.7
528	100-110	<b>1</b>	0	0	76	0	0	13	
529	100-110	12	80	84	116	0	24	60	1.0
	200-210	48	<b>184</b>	60	96	12	28	<b>172</b>	3.0
534	50-60	6	88	66	90	22	20	34	1.3
536	100-110	26	162	<b>102</b>	138	22	0	85	1.6
537	100-110	62	106	95	82	0	0	330	1.1
538	<b>100-110</b>	<b>17</b>	130	72	92	0	0	79	1.8
	200-210	27	<b>186</b>	88	158	28	26	79	2.1
539	100-110	1628	946	58	100	0	0	1556	16.1
540	100-110	16	224	100	228	24	48	35	2.3
	204-214	16	130	72	118	22	26	63	1.8
545	100-110	51	56	48	50	0	0	480	1.2
	200-210	83	42	38	34	0	0	1070	1.2
548	96-106	28	64	50	0	0	0	244	1.3
549	42-51	1	<b>0</b>	0	0	0	<b>0</b>		

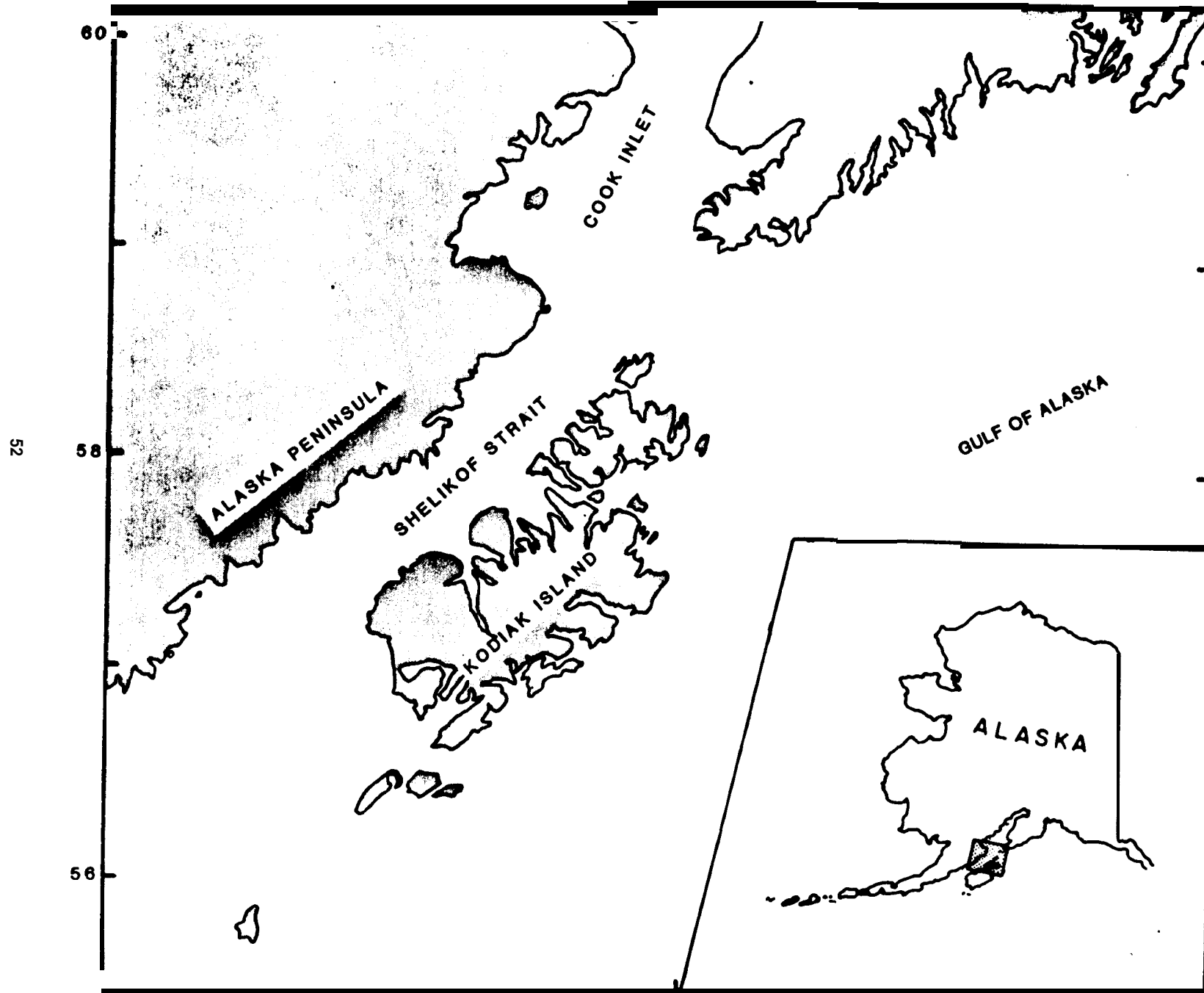
Table 6 cont.

Station	Depth in core (cm)	C <sub>1</sub>	C <sub>2</sub>	<sup>c</sup> <sub>2</sub> :1	C <sub>3</sub>	i-C <sub>4</sub>	n-C <sub>4</sub>	<u>C<sub>1</sub></u>	<u>C<sub>2</sub></u>
		Methane (μl/l)	Ethane (nl/l)	Ethene (nl/l)	Propane (nl/l)	Isobutane (nl/l)	n-butane (nl/l)	<u>C<sub>2</sub>+C<sub>3</sub></u>	<u>c<sub>2</sub>.1</u>
550	100-110	28	64	50	54	0	0	244	1.3
	200-210	17	42	26	54	18	24	180	1.6
551	<b>91-101</b>	30	<b>154</b>	82	126	20	16	107	1*9
552	50-60	18	44	36	36	0	0	231	1.2
	100-110	14	24	<b>18</b>	62	0	0	165	0.4

FIGURE CAPTIONS

1. Location map of the study area in Shelikof Strait
- 2\* **Tracklines** of continuous seismic reflection profiles and locations of sampling stations (numbered). Solid lines represent the 1979 Nekton survey contracted by the USGS Conservation Division, and dashed lines represent the 1980 R/V S.P. LEE cruise.
3. Bathymetry of **Shelikof** Strait, 5-m contour interval. Depths corrected to mean lower low water.
4. Shallow structures. Bold lines represent fault offset of the seafloor (hachures on downthrown side), dashed lines indicate buried faults that offset unconsolidated sediment, and dotted lines indicate uncertain extent of buried faults. Fold axes (from **Hoose** and Whitney, 1980) denoted by narrow lines.
5. **Boomer** seismic reflection profile showing high-offset faults.
6. Thickness of near-surface sedimentary units of probable Pleistocene and younger age. Contour interval: 25 milliseconds of two-way travel time, except 100 ms for dotted contours where data are relatively sparse and contours are generalized.
7. Seismic reflection record across marginal channel.
8. Pie-diagrams showing relative abundances of textural classes in sediment samples.
9. Mean grain size of seafloor sediment, in phi-units.
10. Vane shear strength (in **kilopascals**) at shallowest level measured in core (typically at 15 cm; none deeper than 74 cm).
11. **Anisotropy** of vane shear strength versus plasticity index, including experimentally derived curve of Bjerrum (1973).  $S_{us}$  is the predicted (from the regression line) value of undisturbed strength measured on a split core, and corrected Sue is the (corrected) value of undisturbed strength measured on an end of core. Both values are hypothetically from the same depth in the core.
12. Sensitivity at shallowest level measured in core (typically at 15 cm; none deeper than 74 cm).
13. Water content at shallowest level measured in core (typically at 15 cm; none deeper than 74 cm).
14. Liquid limit at shallowest level measured in core (typically at 15 cm; none deeper than 129 cm).

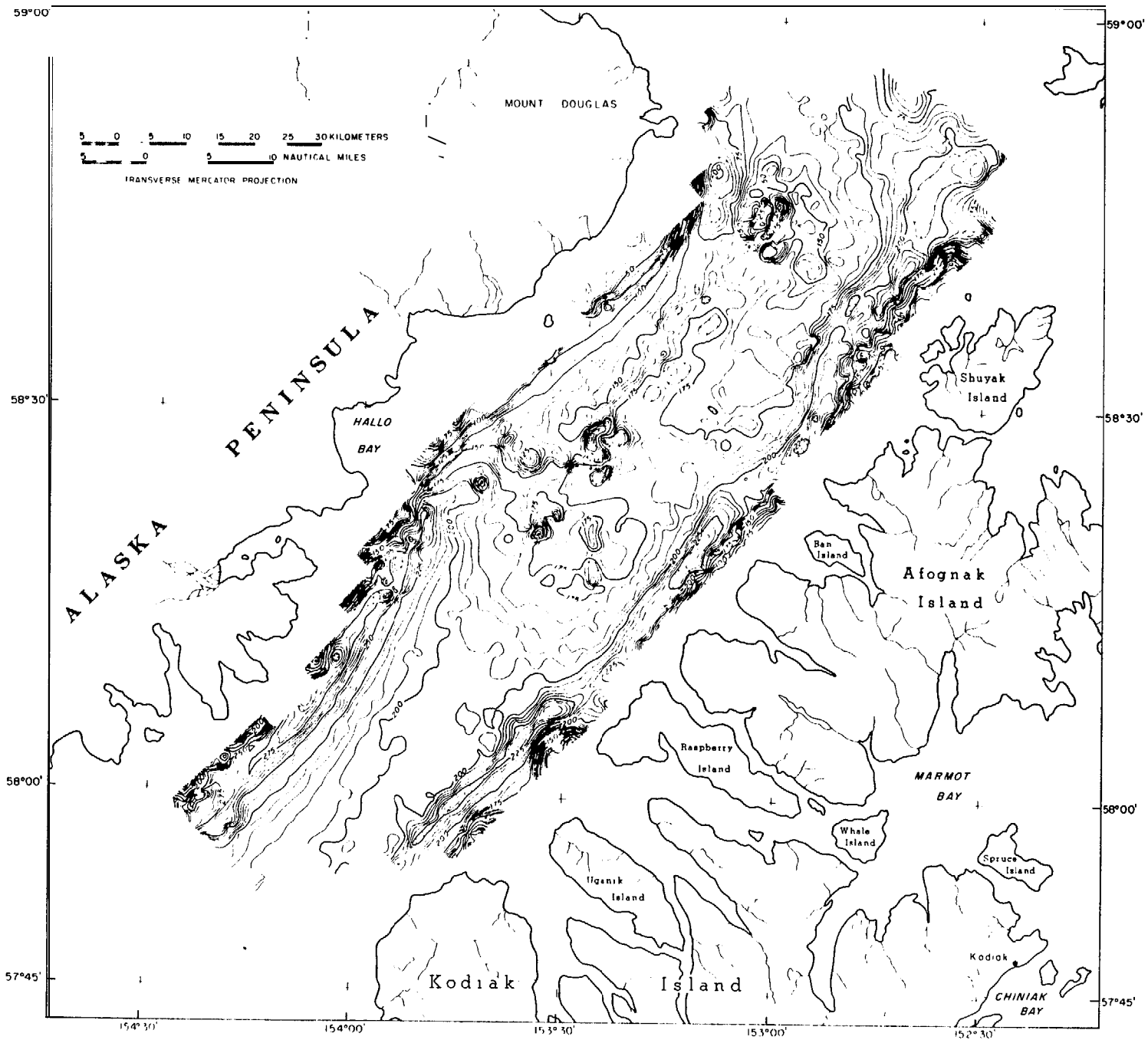
15. Plastic limit at shallowest level measured in core (typically at 15 cm; none deeper than 129 cm).
16. Plasticity index at shallowest **level** measured in core (typically at 15 cm; none deeper than 129 cm)
- 17. Liquid limit versus mean grainsize.**
18. Plastic limit versus mean grain size.
19. Plasticity versus mean grain size.
20. Plasticity chart.
21. Organic carbon (percent dry weight) in seafloor sediment.
22. Carbonate carbon (percent dry weight) in seafloor sediment.
23. Organic carbon versus grain size.
24. Water content versus organic carbon.
25. Plasticity index versus organic carbon.
26. Shear strength versus organic carbon.
27. Sensitivity versus organic carbon.
28. Liquidity index versus organic carbon.
29. **Illite** content of seafloor sediment.
30. Chlorite content of seafloor sediment.
31. Mixed-layer clay (mostly **smectite**) content of seafloor sediment.
32. Locations of acoustic anomalies along **tracklines**.
33. **Uniboom** seismic reflection record showing acoustic anomaly over truncated fold in bedrock. Vertical scale is in two-way travel time.
34. Locations of craters along **tracklines**. Dots represent seafloor craters; circles represent buried craters.
35. **Uniboom** seismic reflection record showing seafloor and buried craters. Vertical scale is in two-way travel time.
36. **Uniboom** seismic reflection record showing slump mass at base of seafloor escarpment. Vertical scale is in two-way travel time.

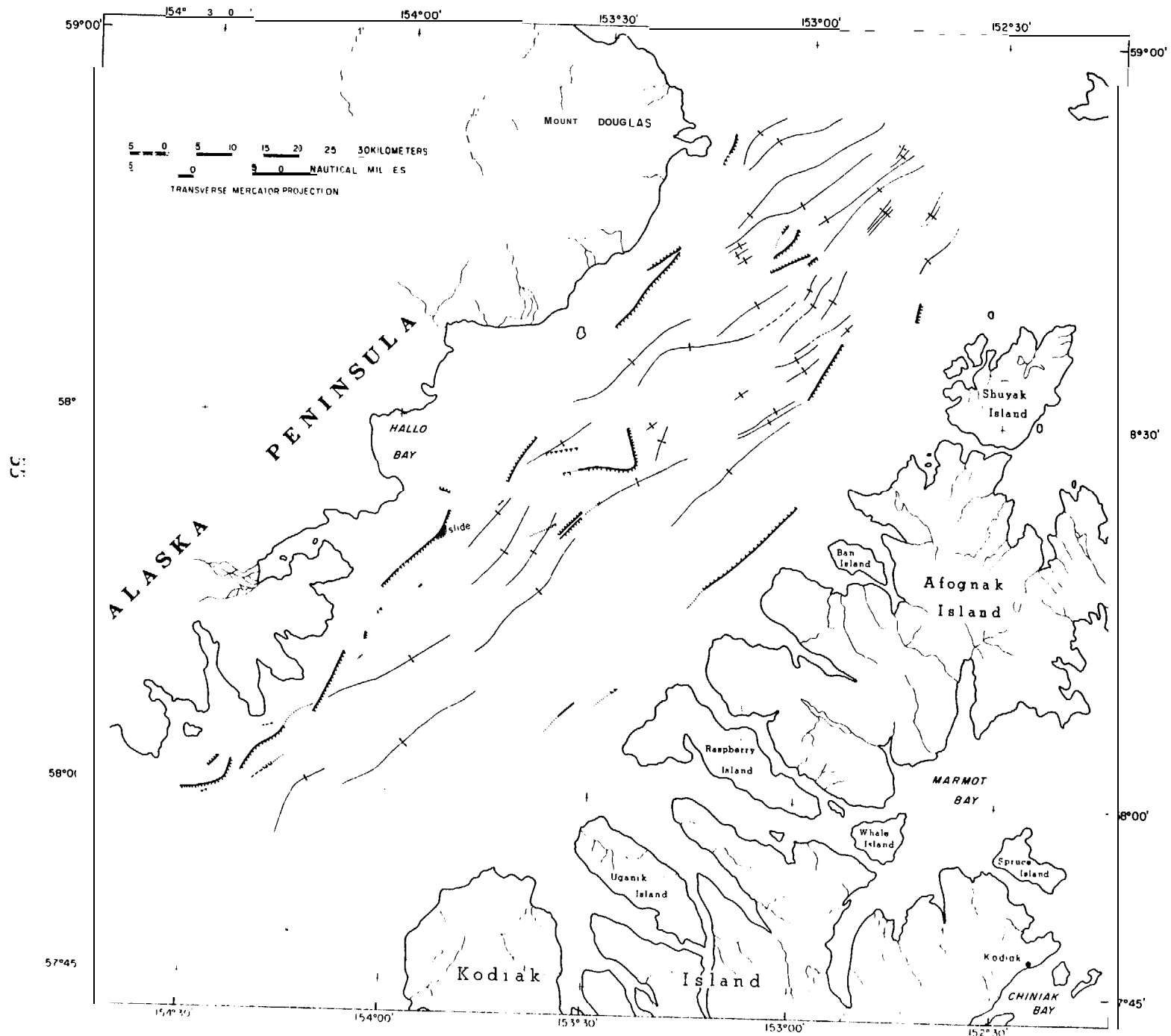


Fig



53





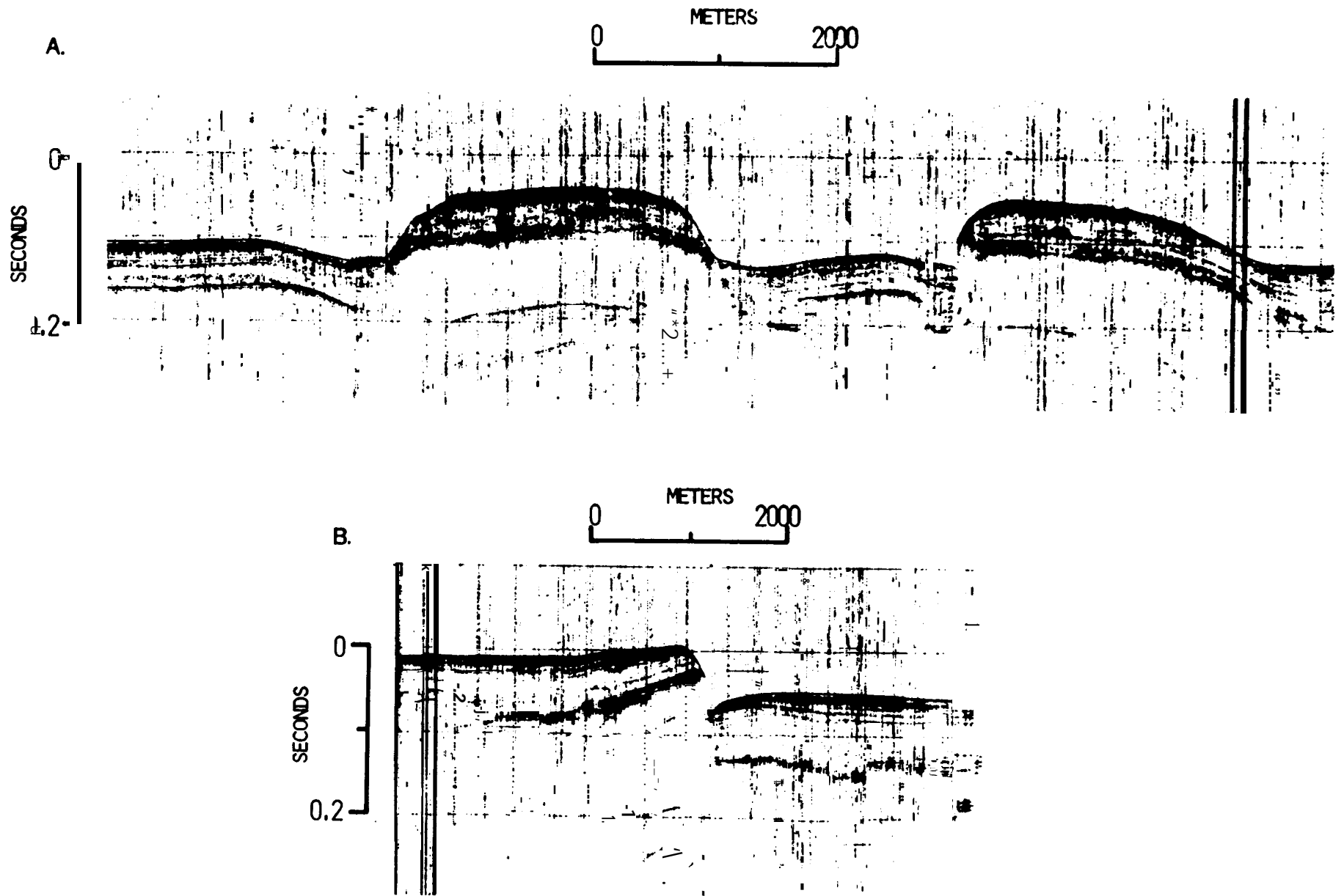


Fig. 5

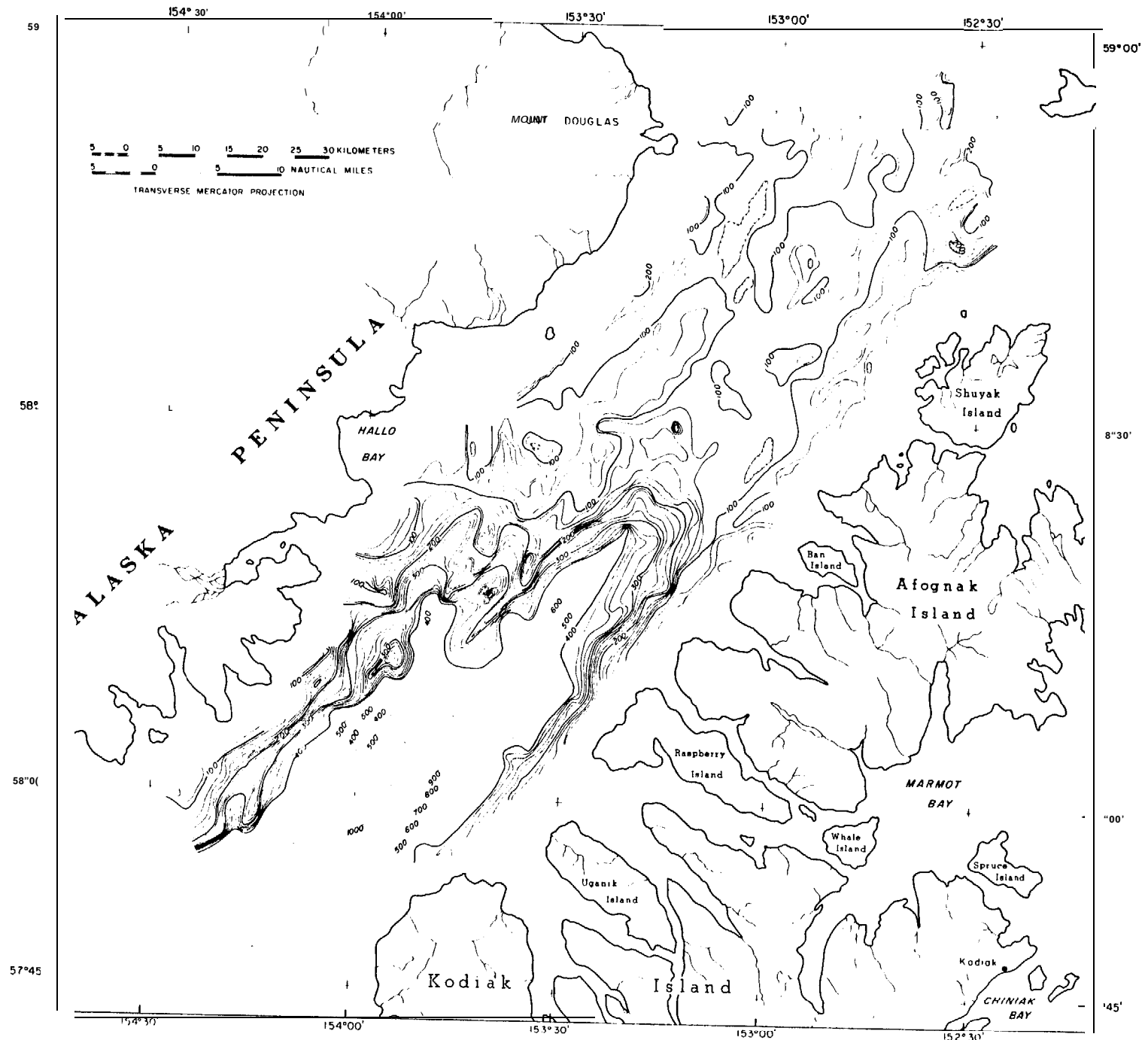


Fig. 1

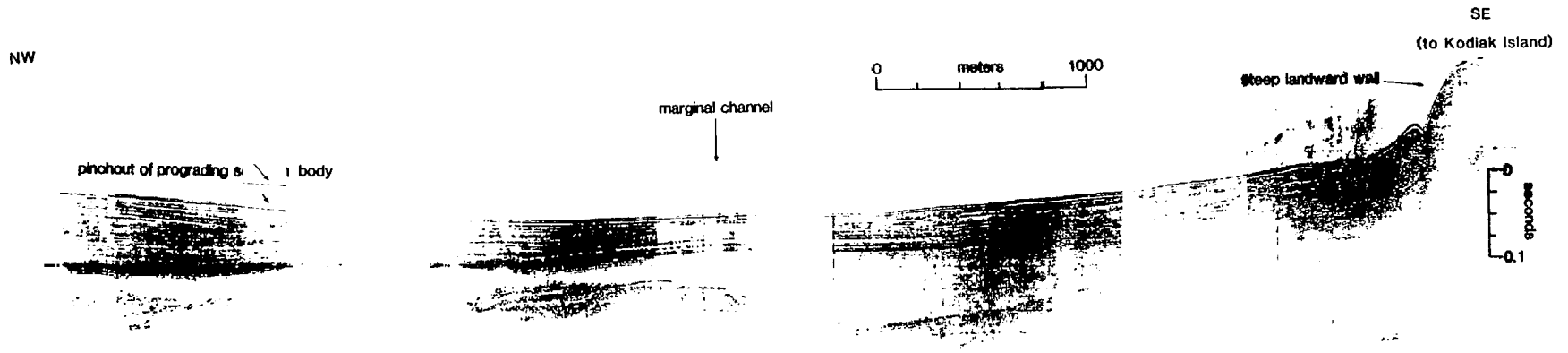


Fig. 7

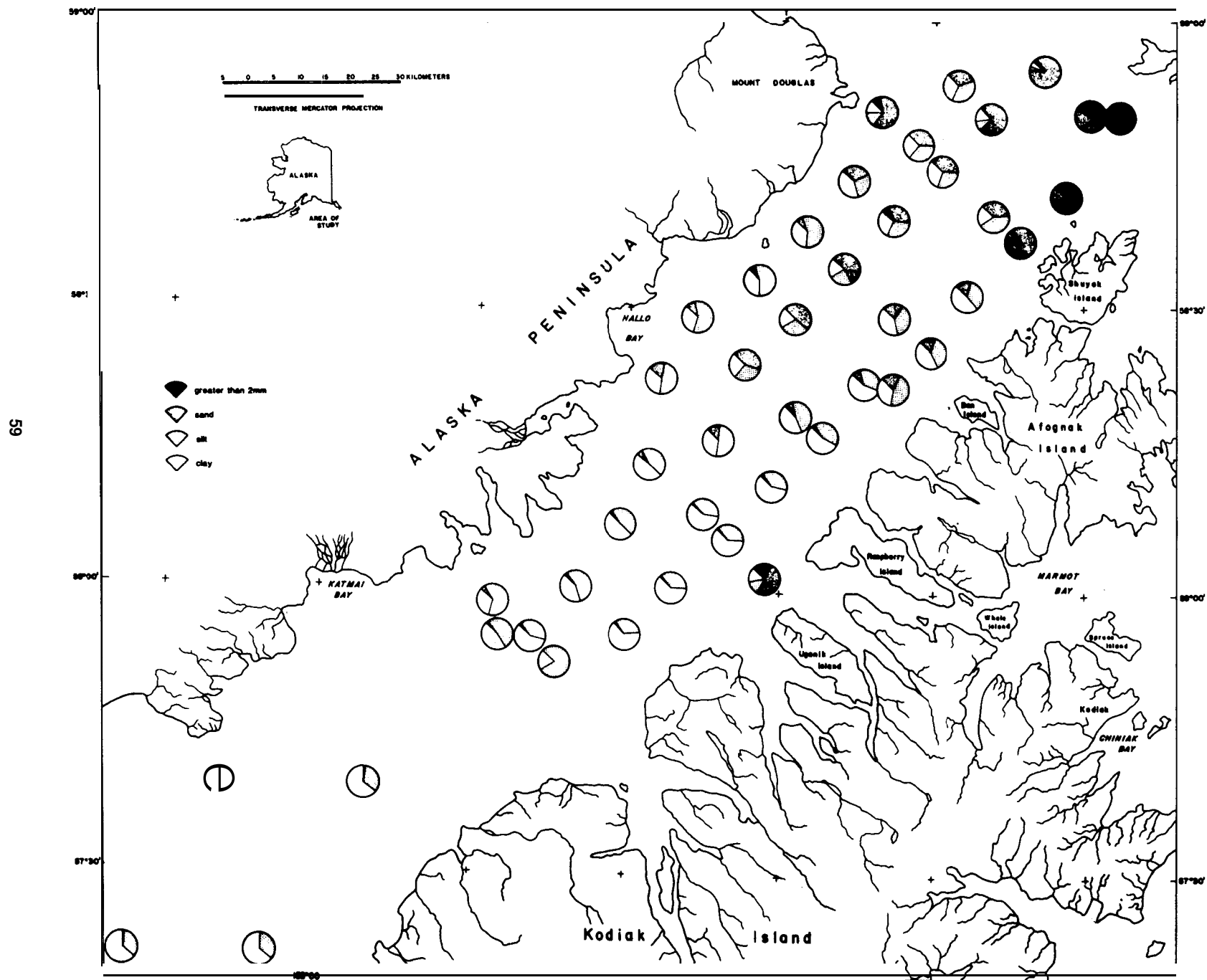


Fig. 8

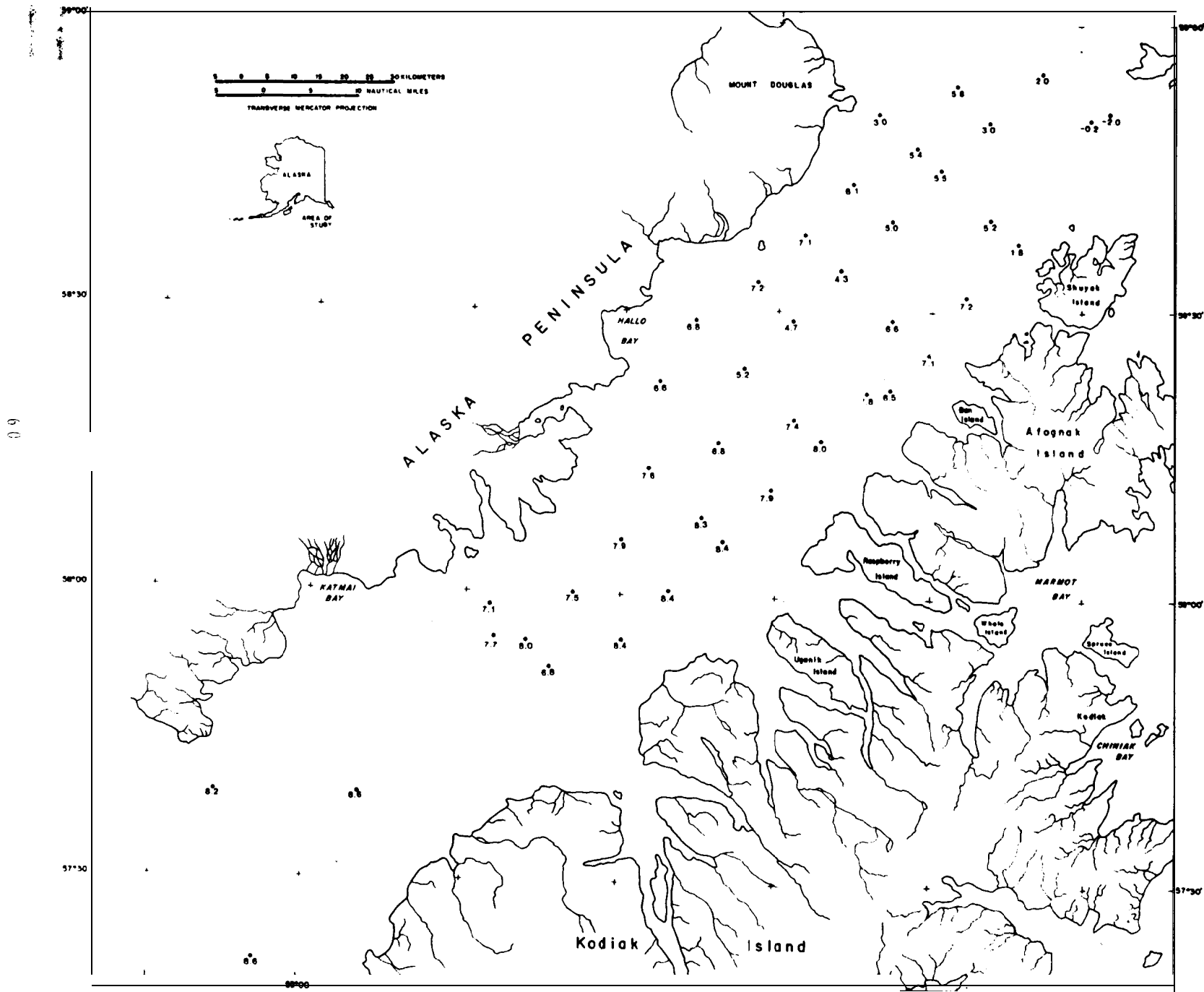


Fig. 9

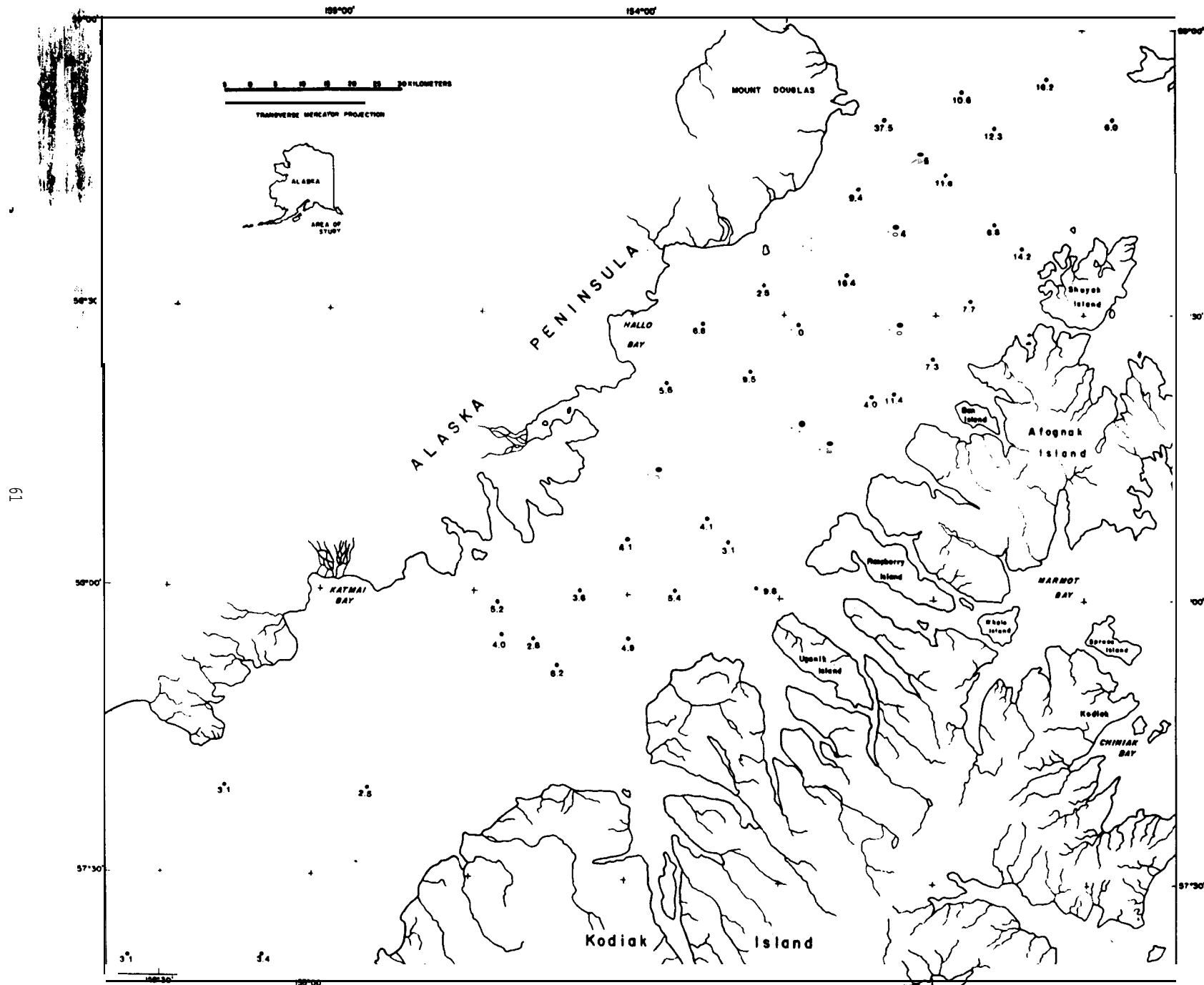


Fig. 10

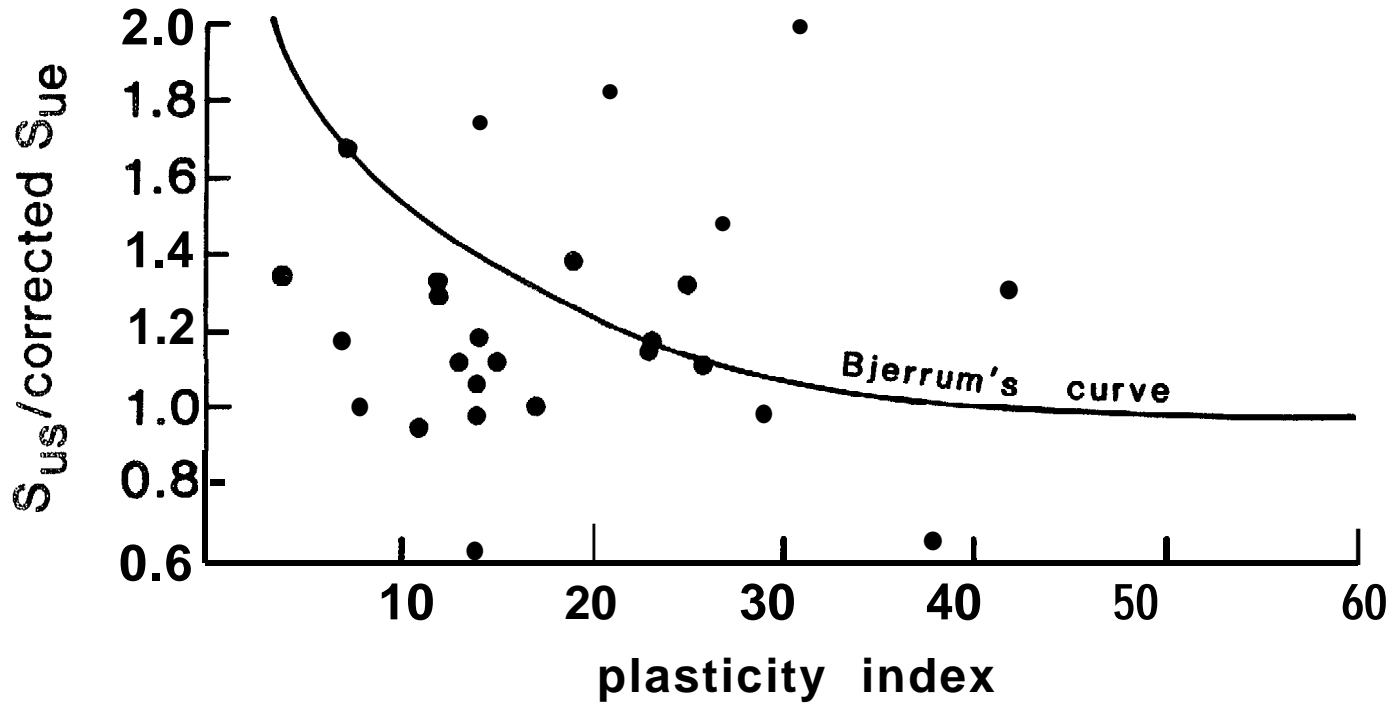


Fig. 11

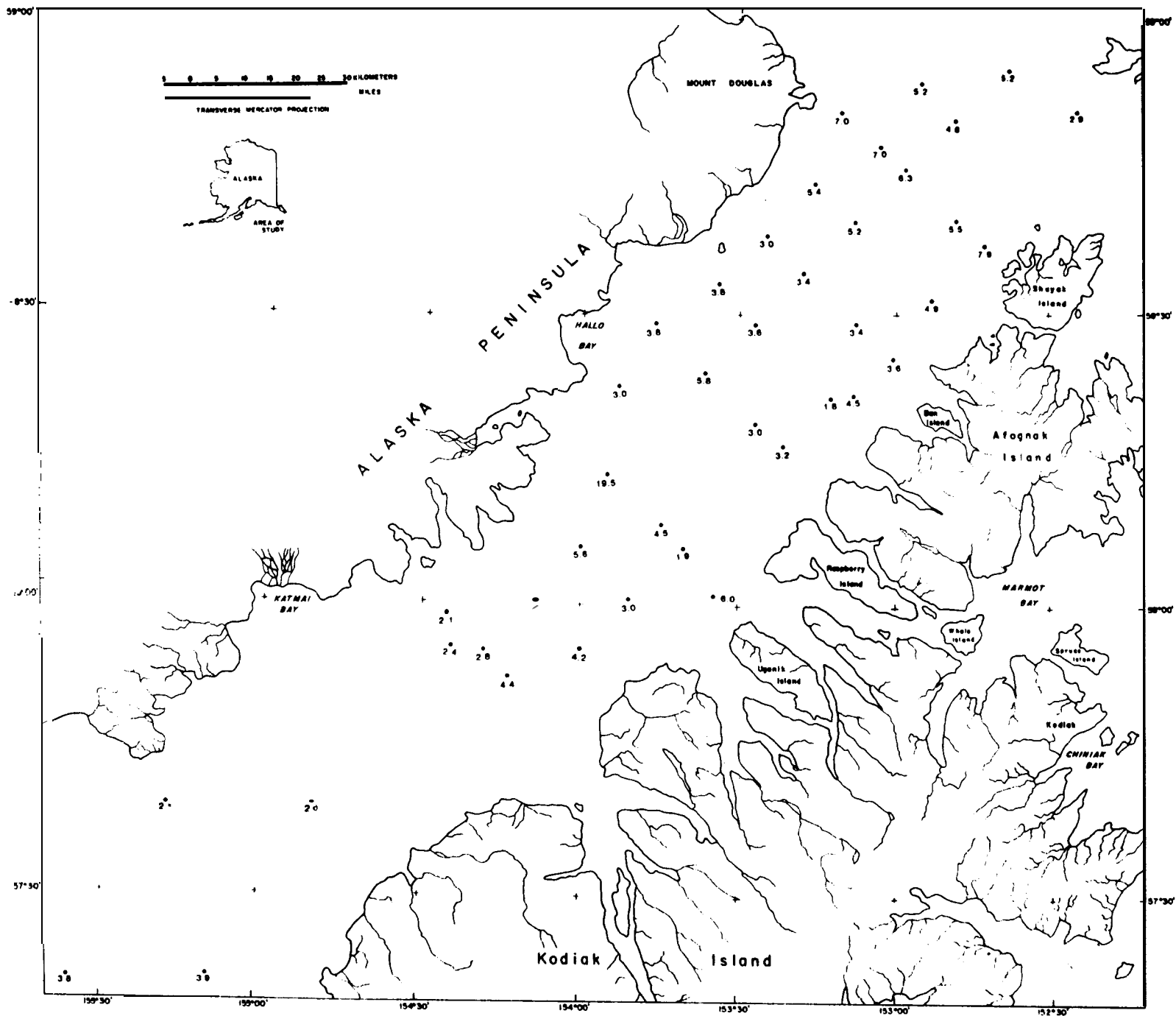
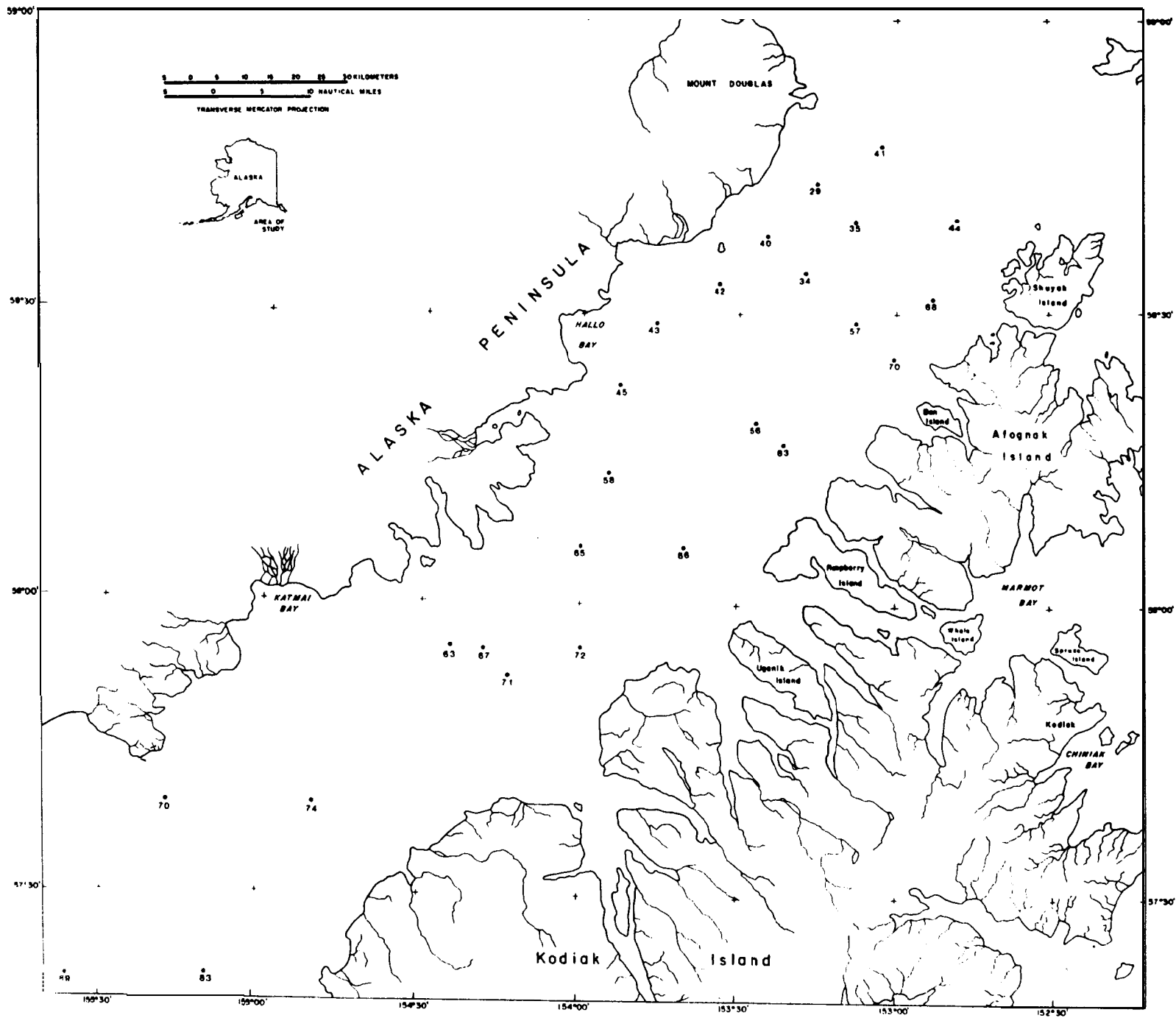


Fig. 12





65

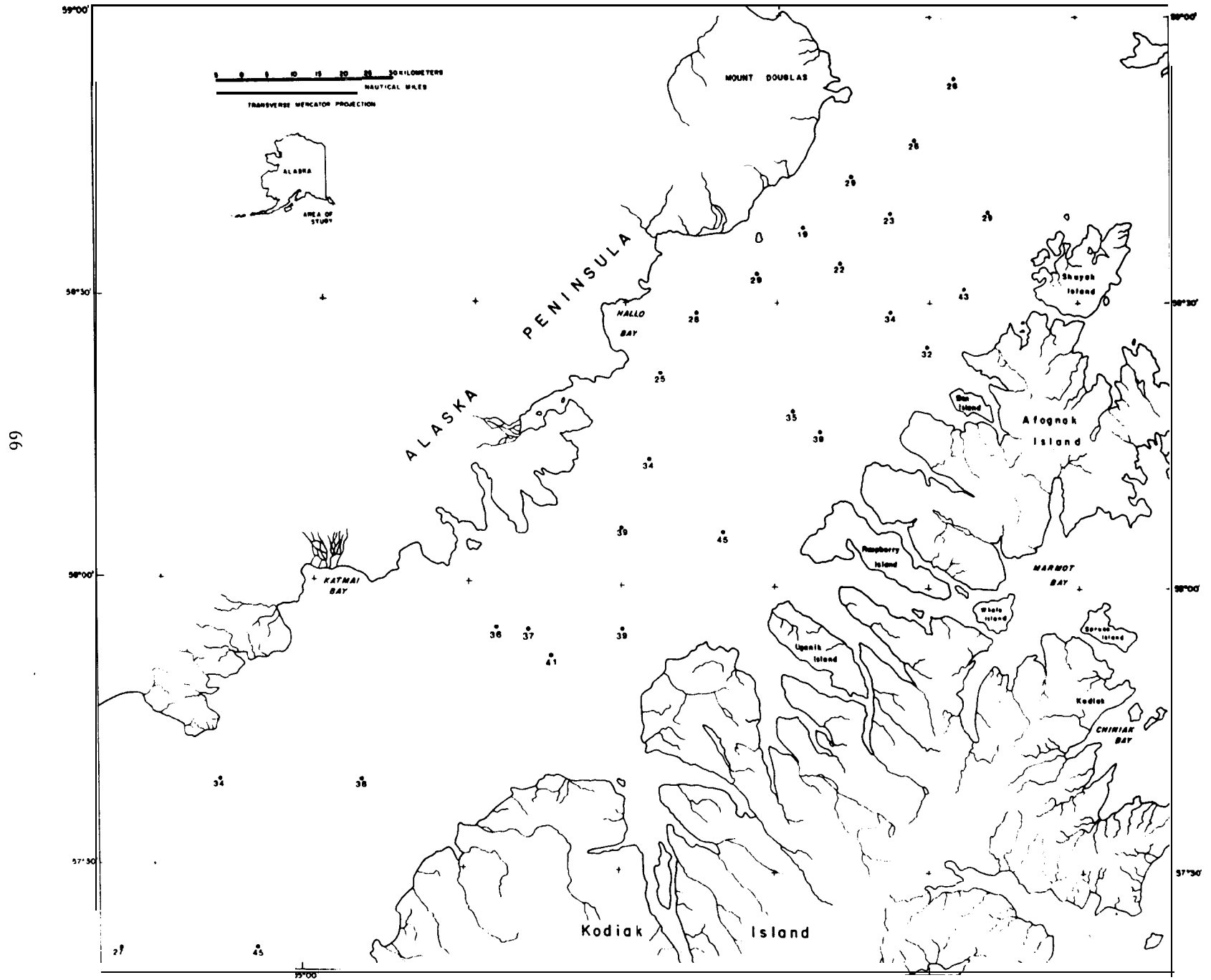


Fig. 15

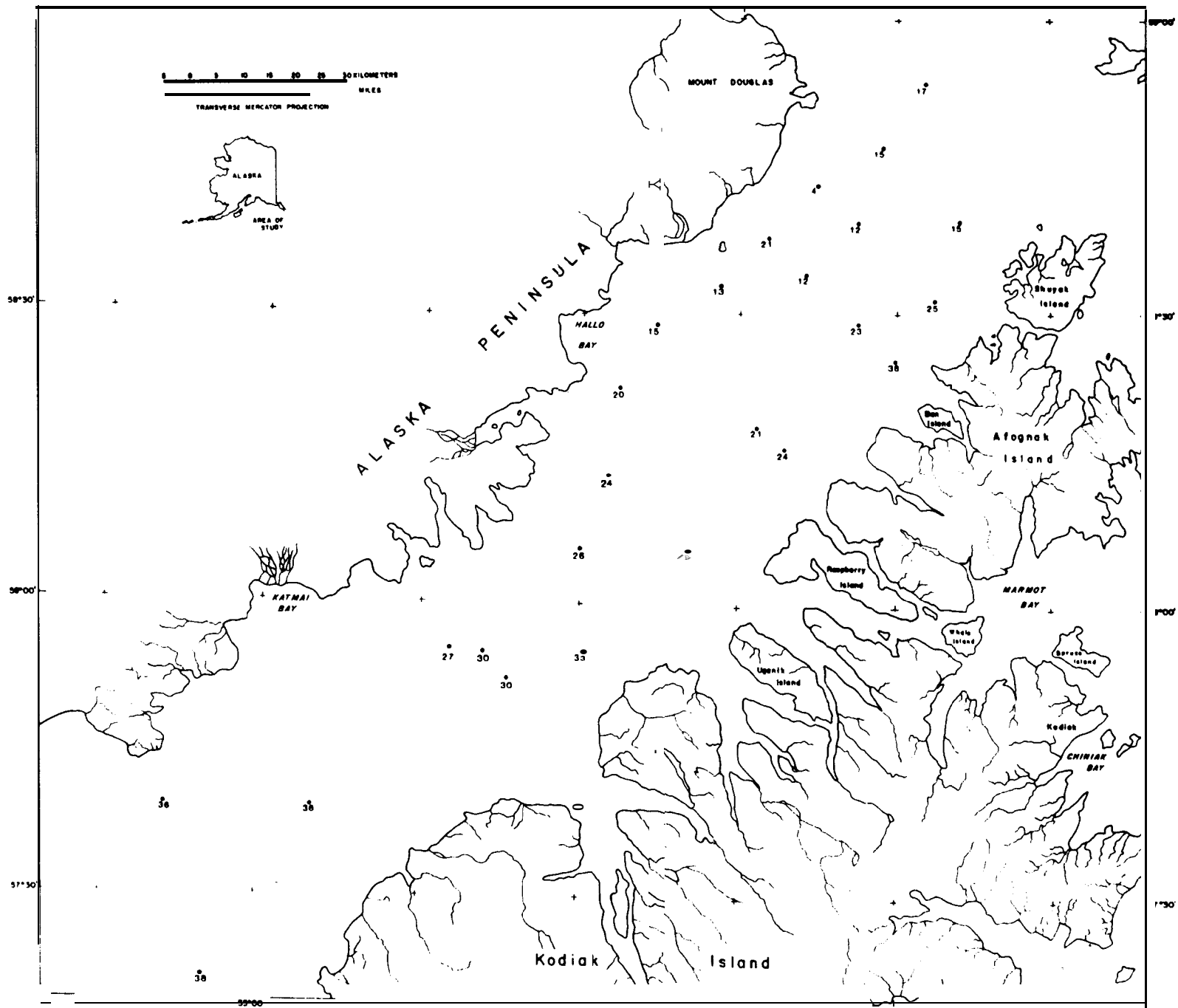


Fig. 16



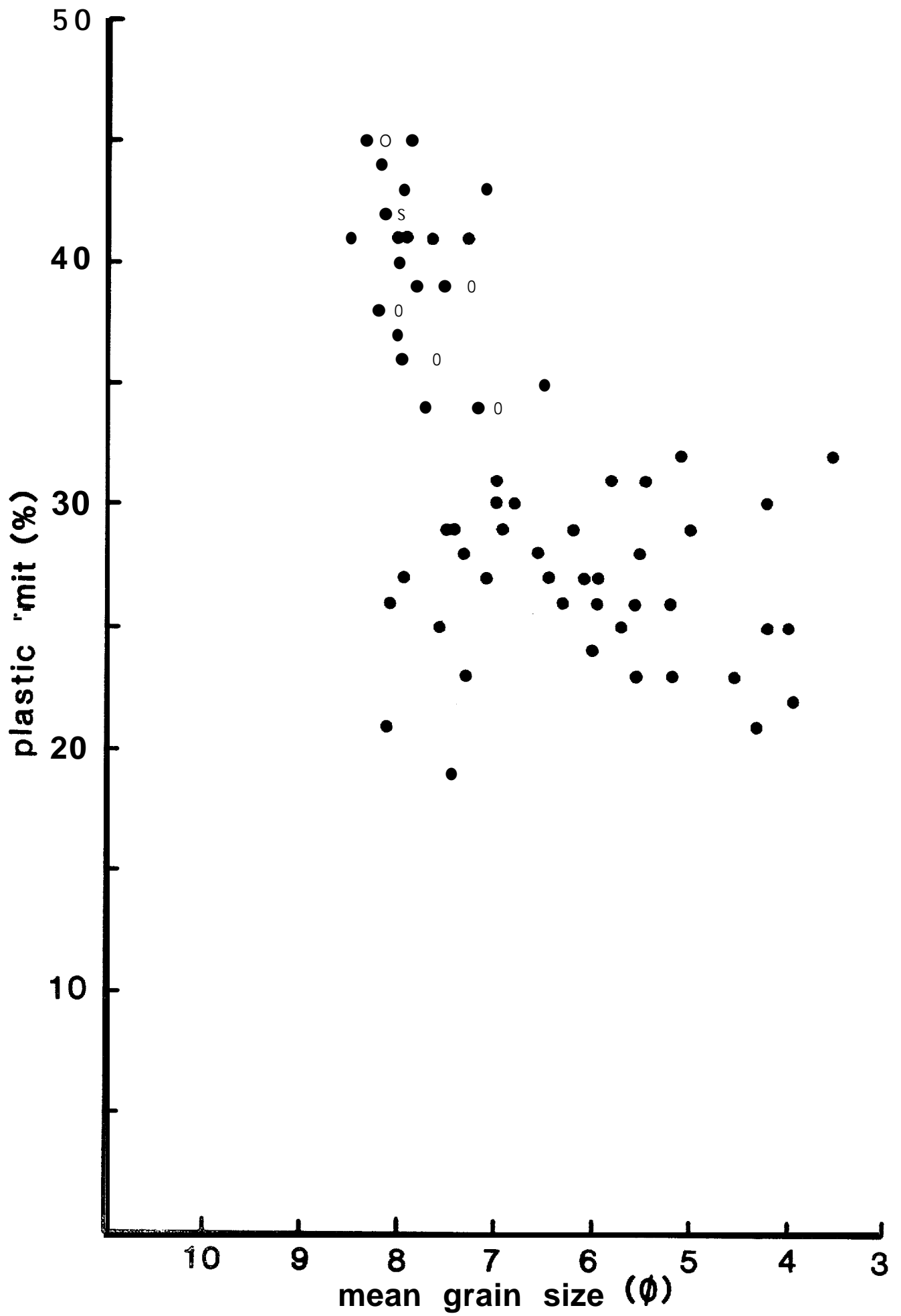
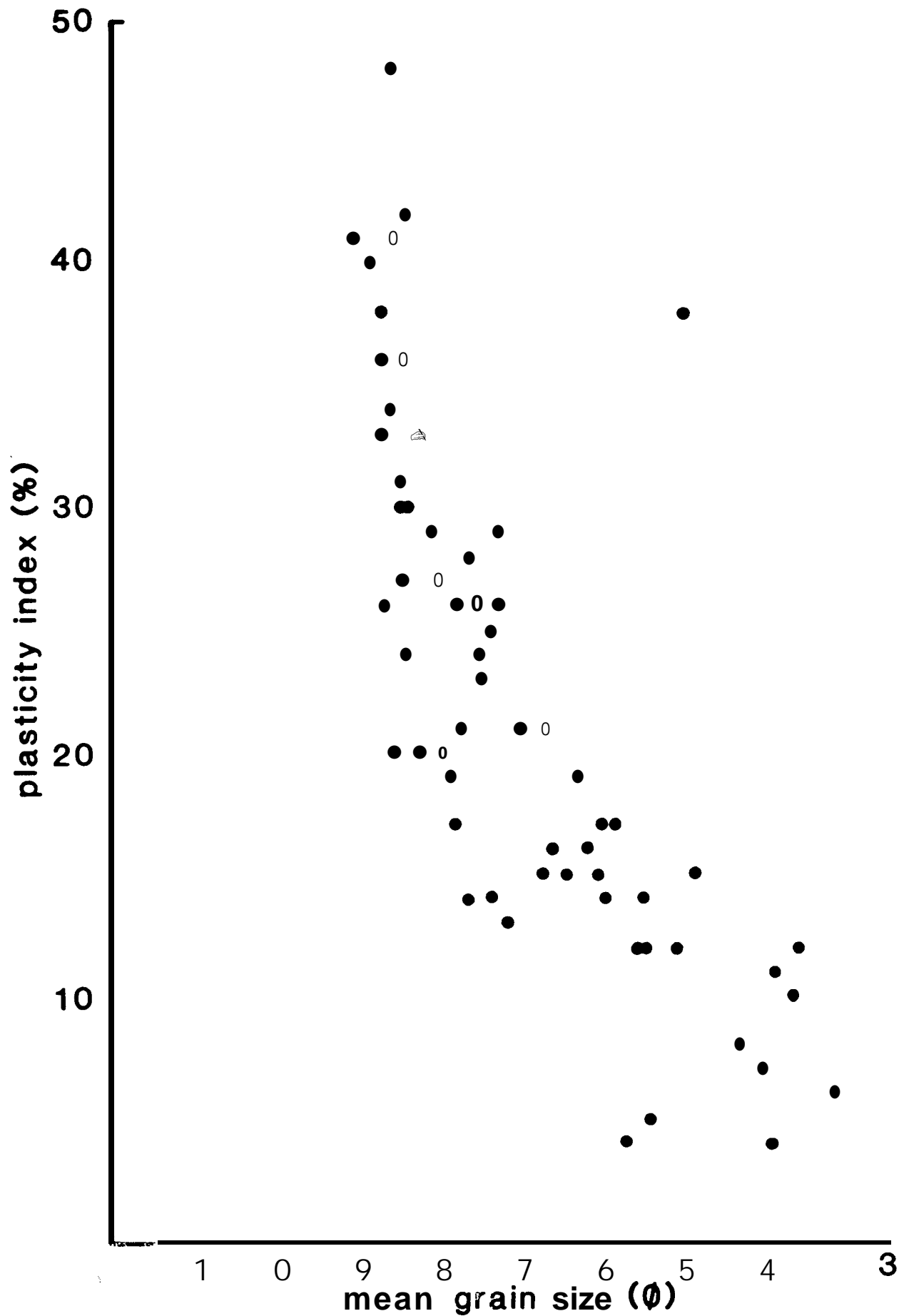


Fig. 18



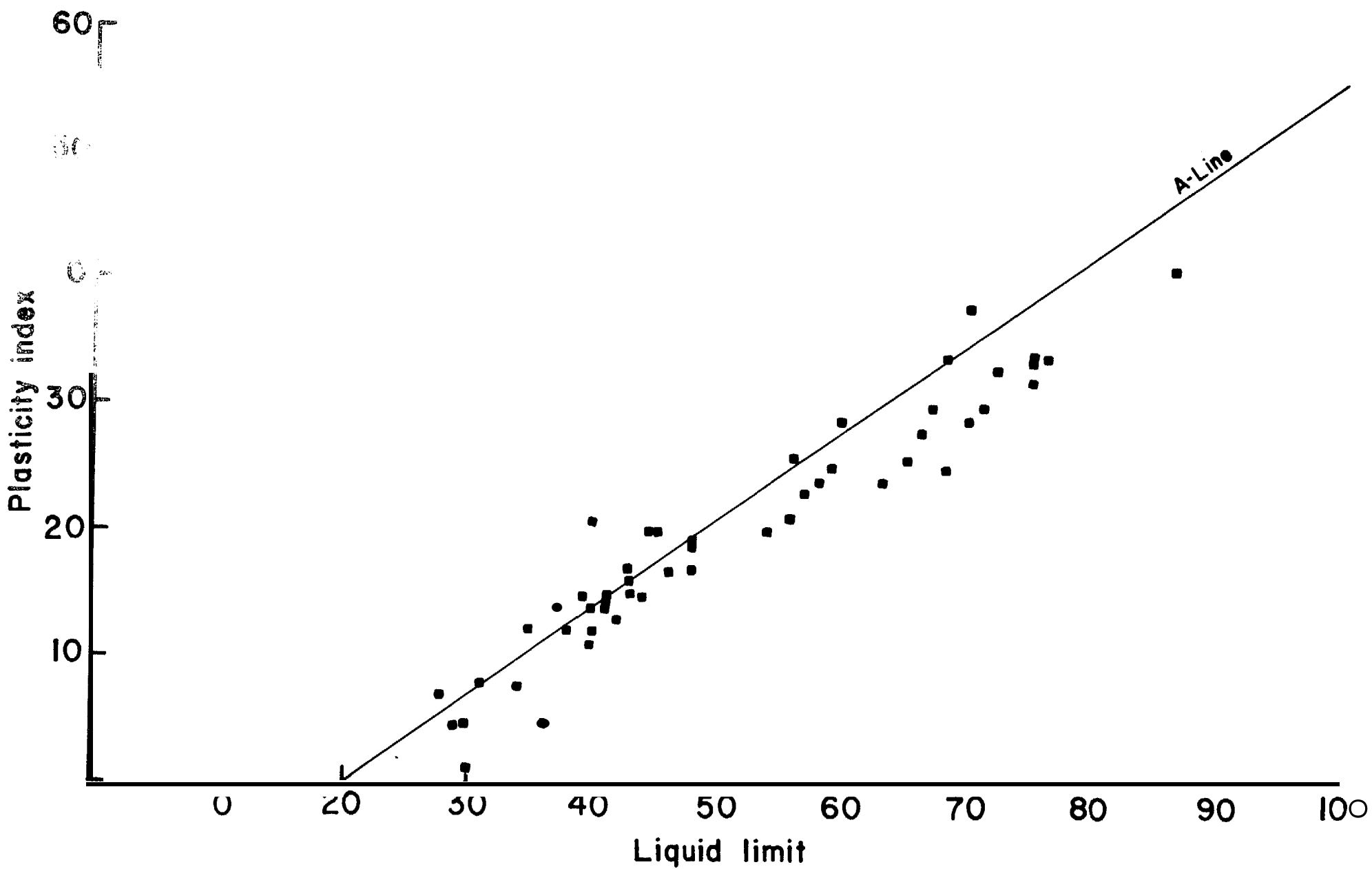
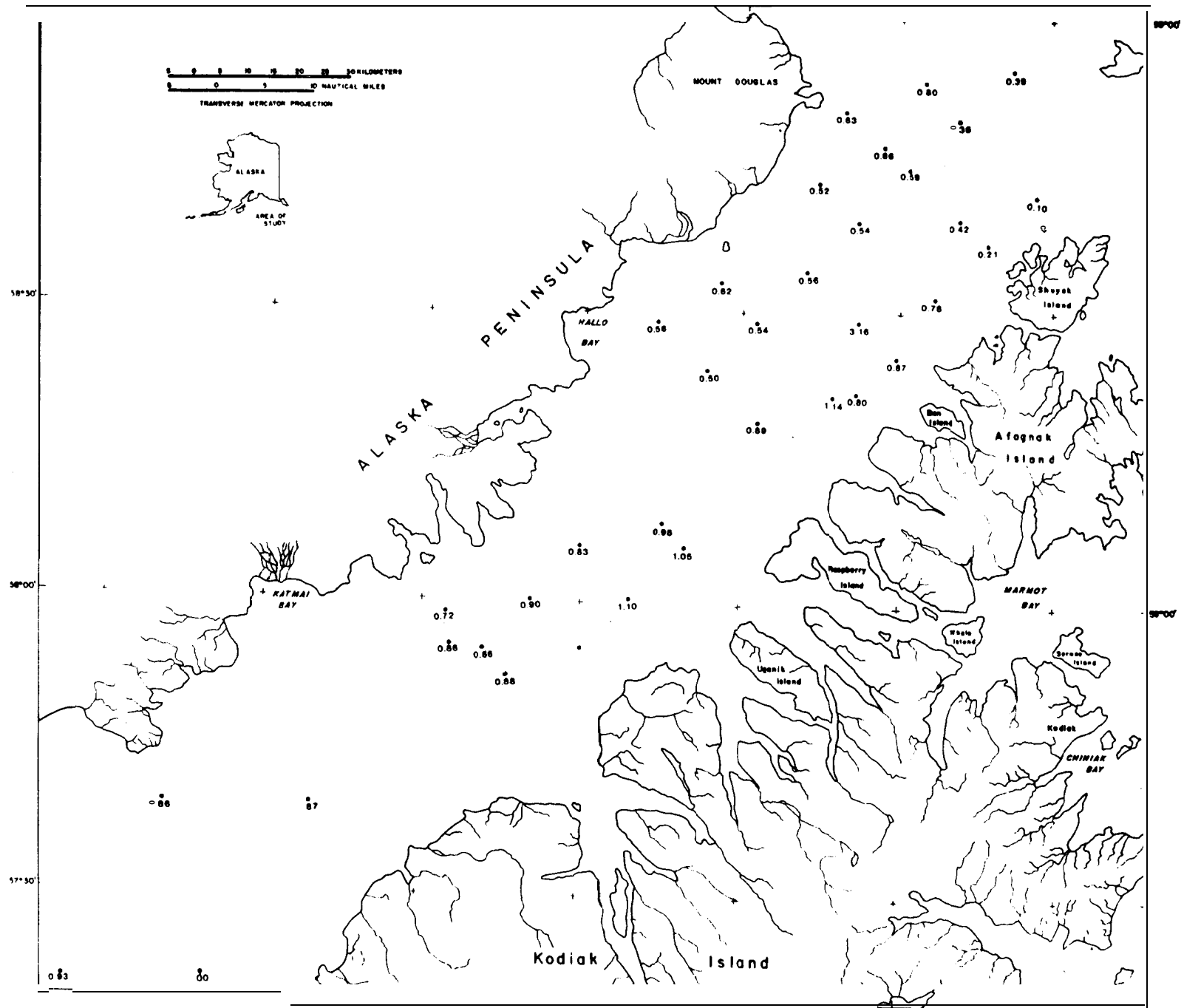
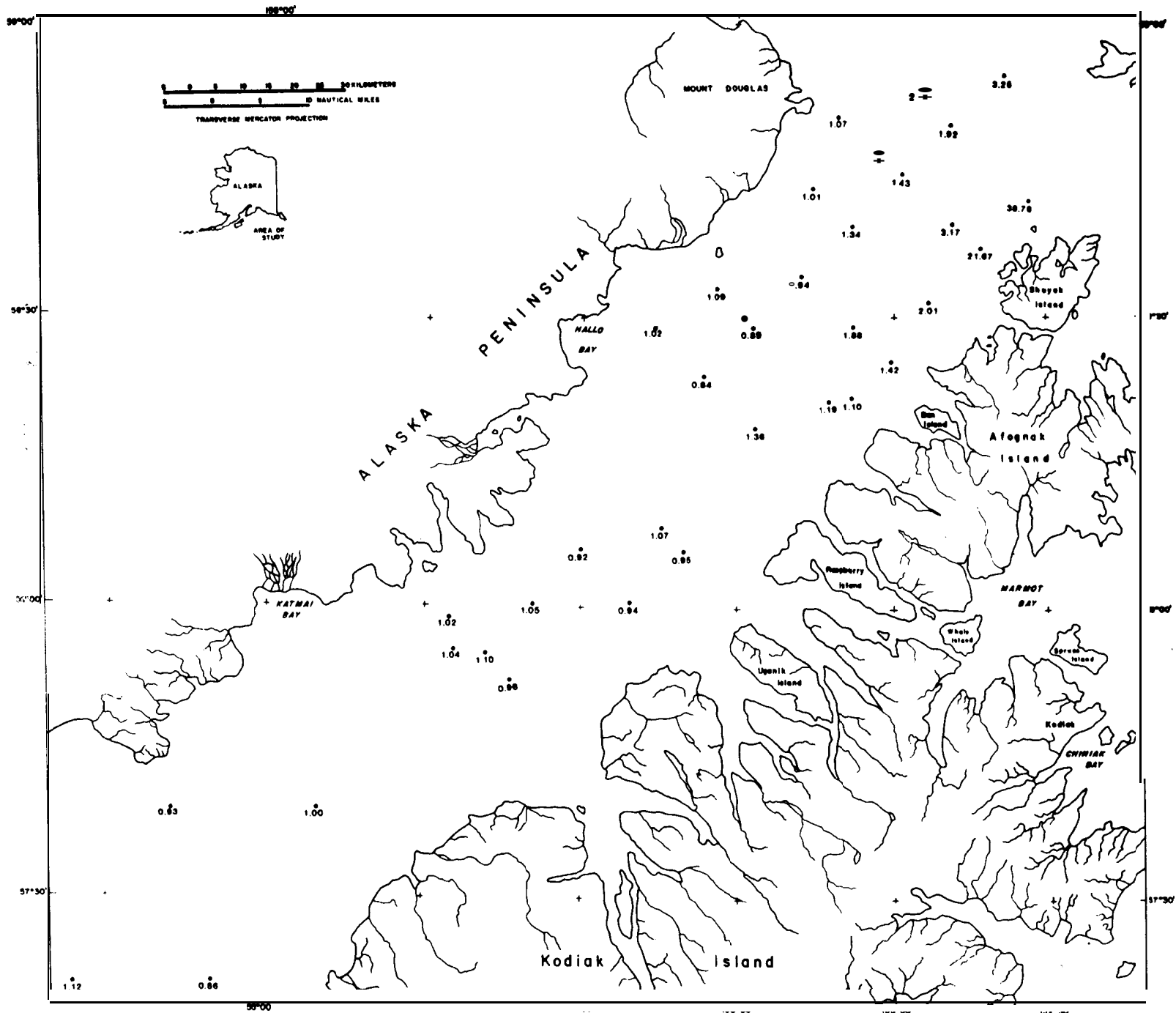


Fig. 2°



72

Fig 21



73

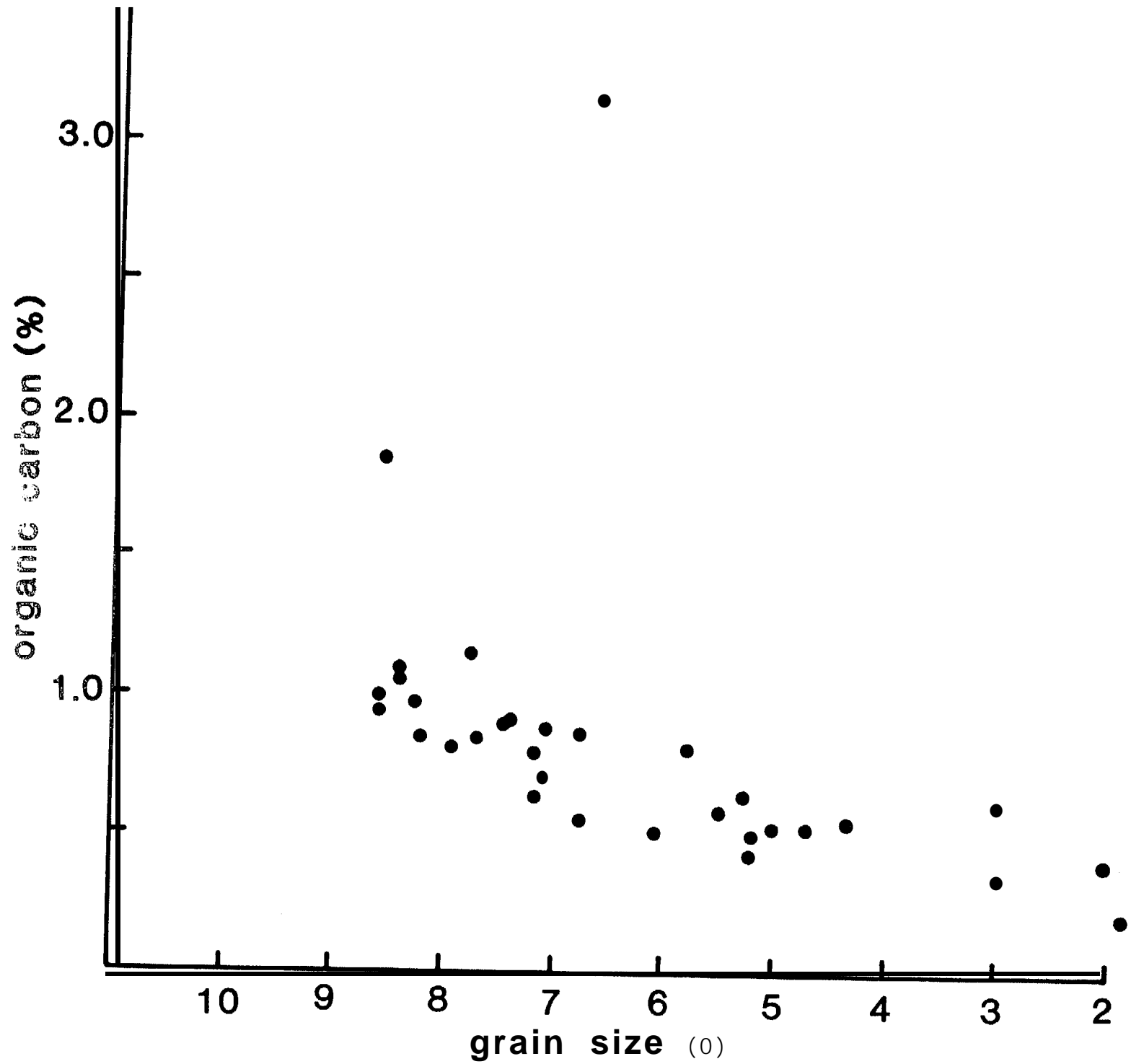


Fig. 23

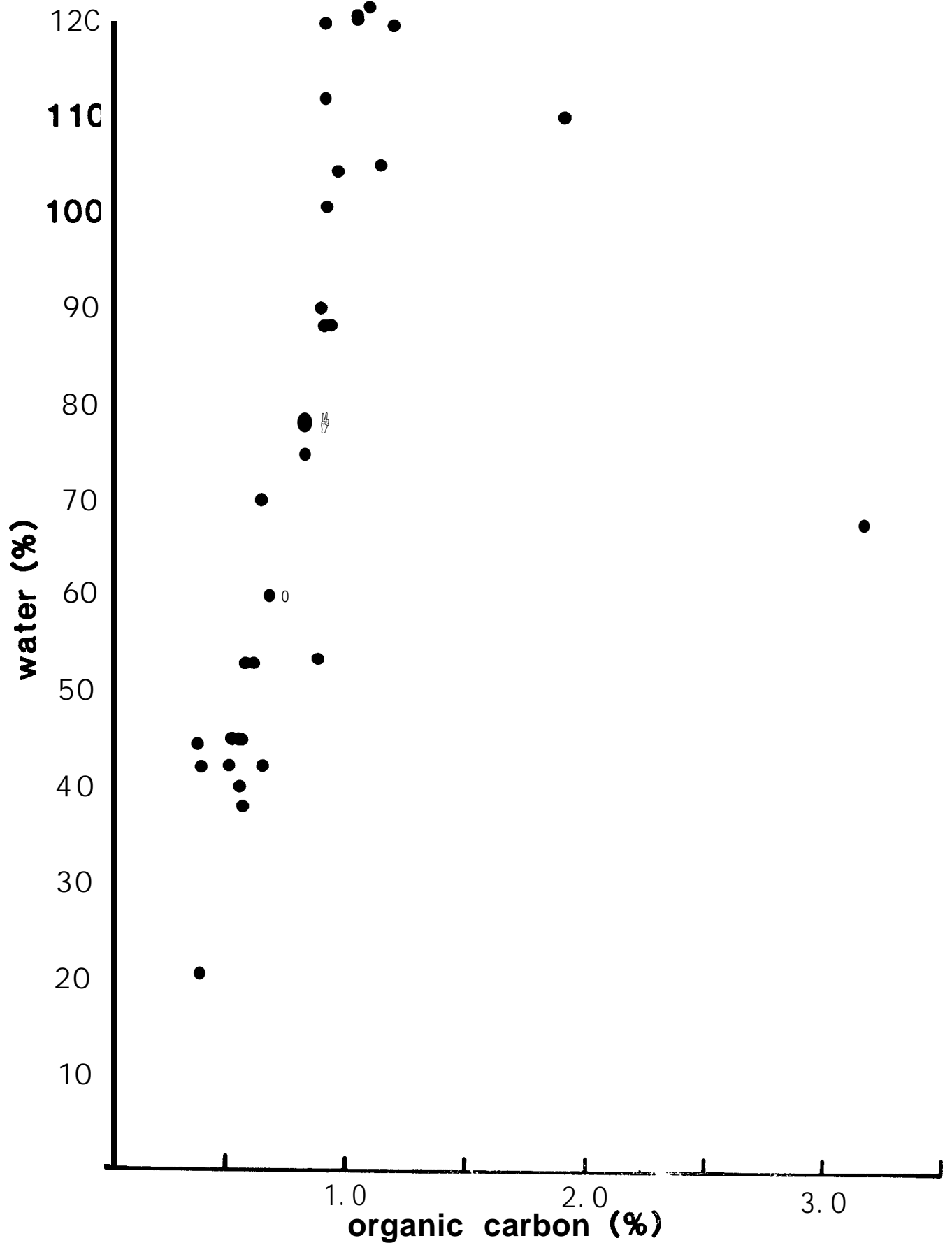


Fig. 24

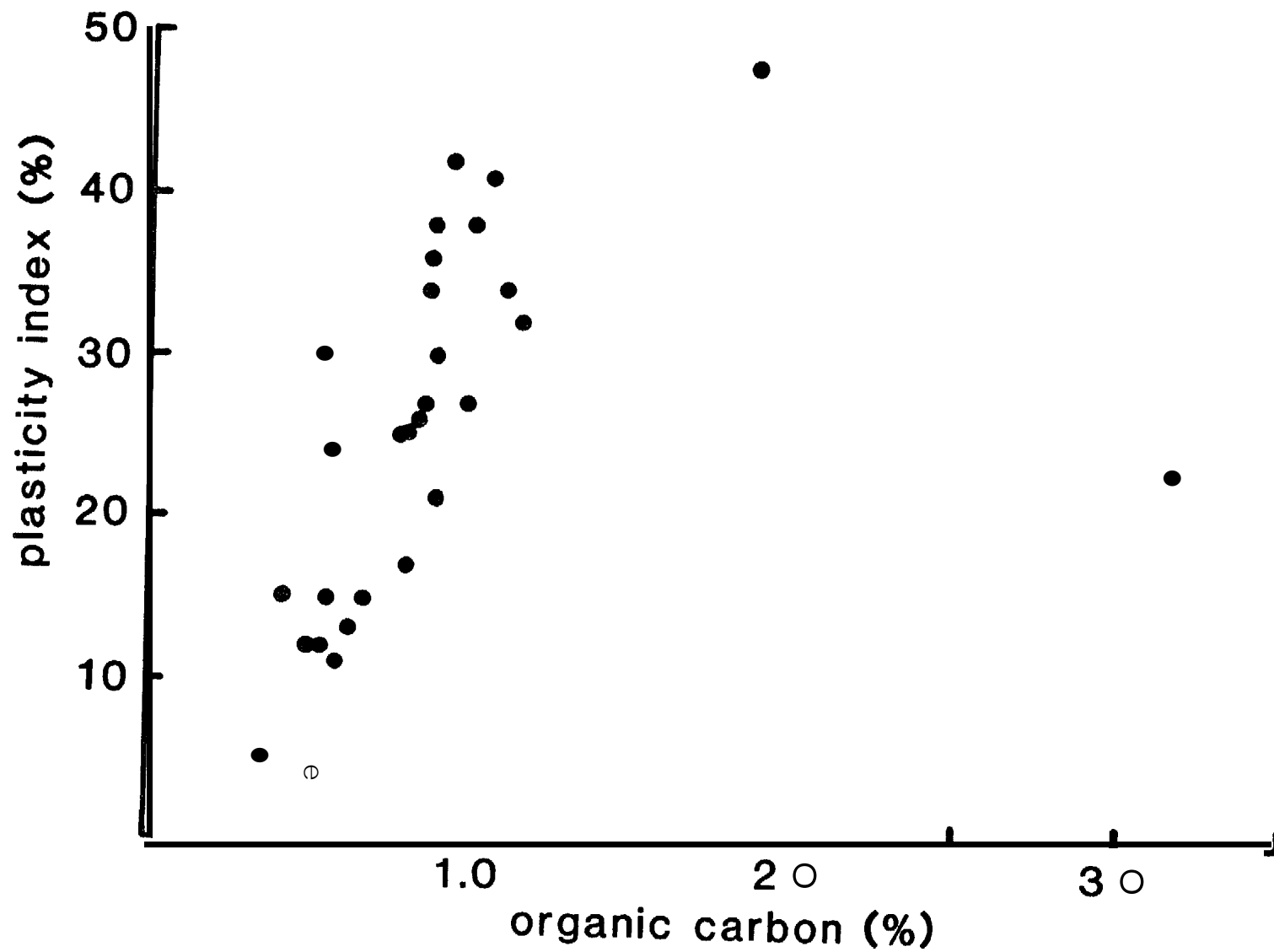


Fig. 25



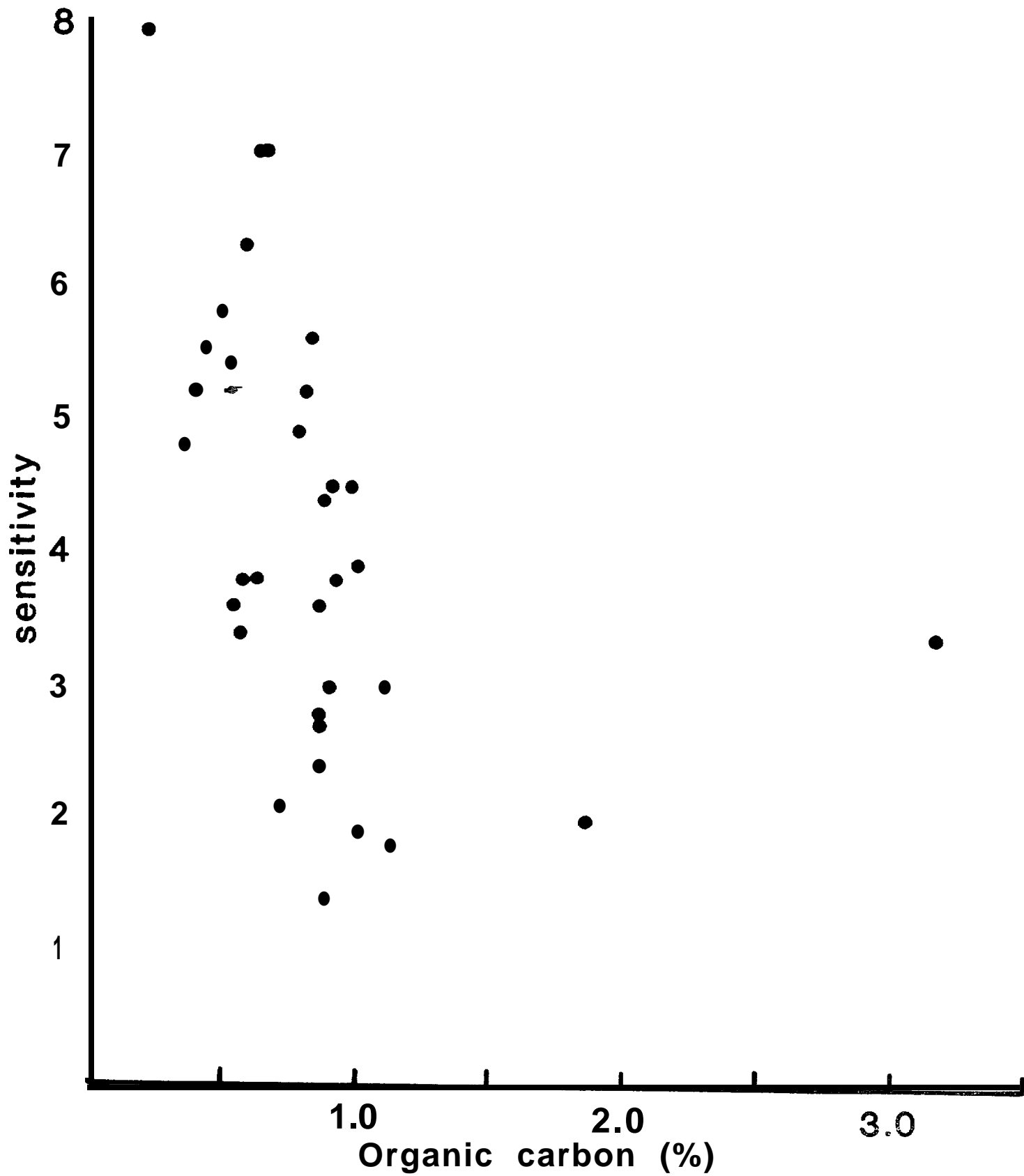


Fig. 27

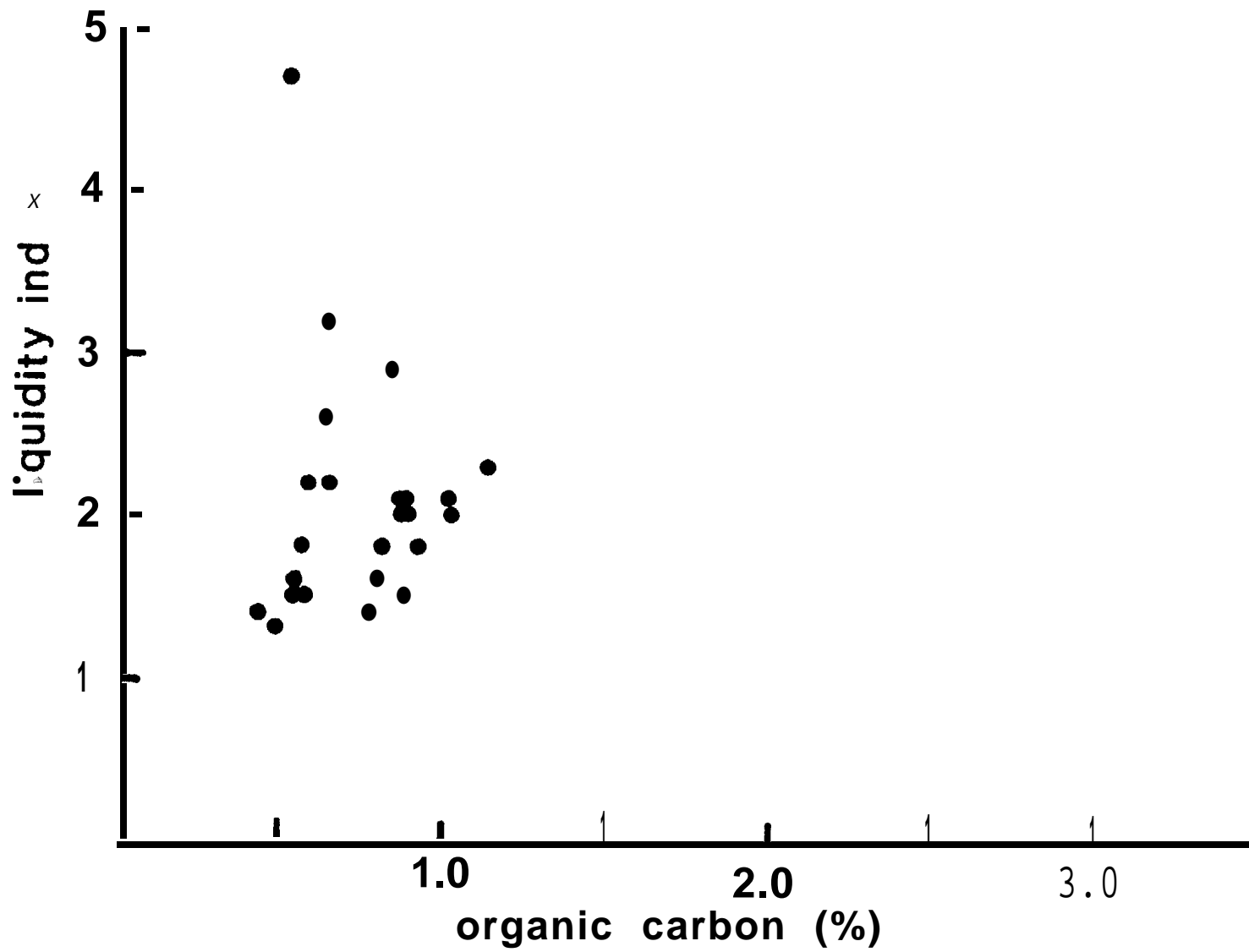


Fig. 28

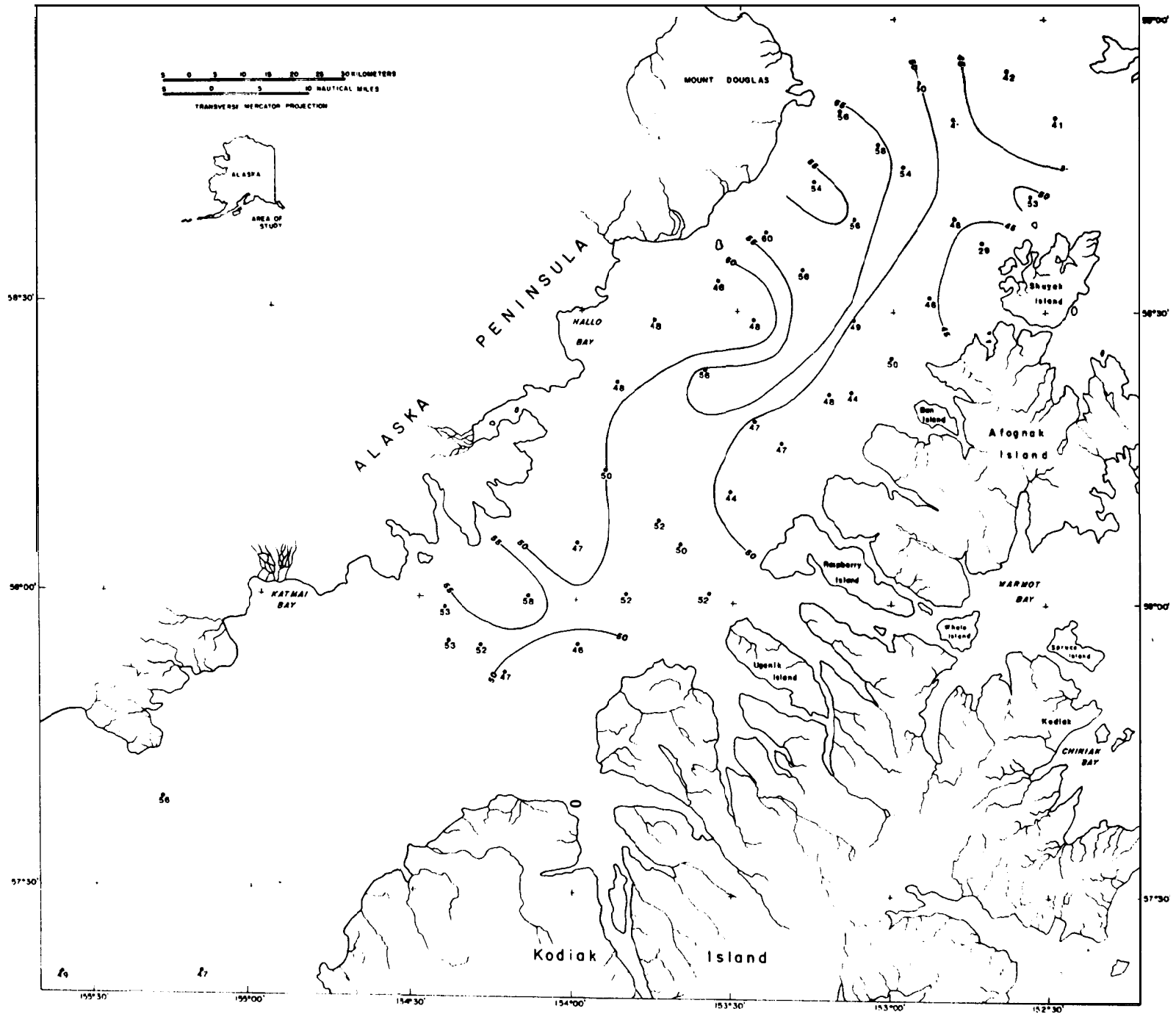


Fig. 29

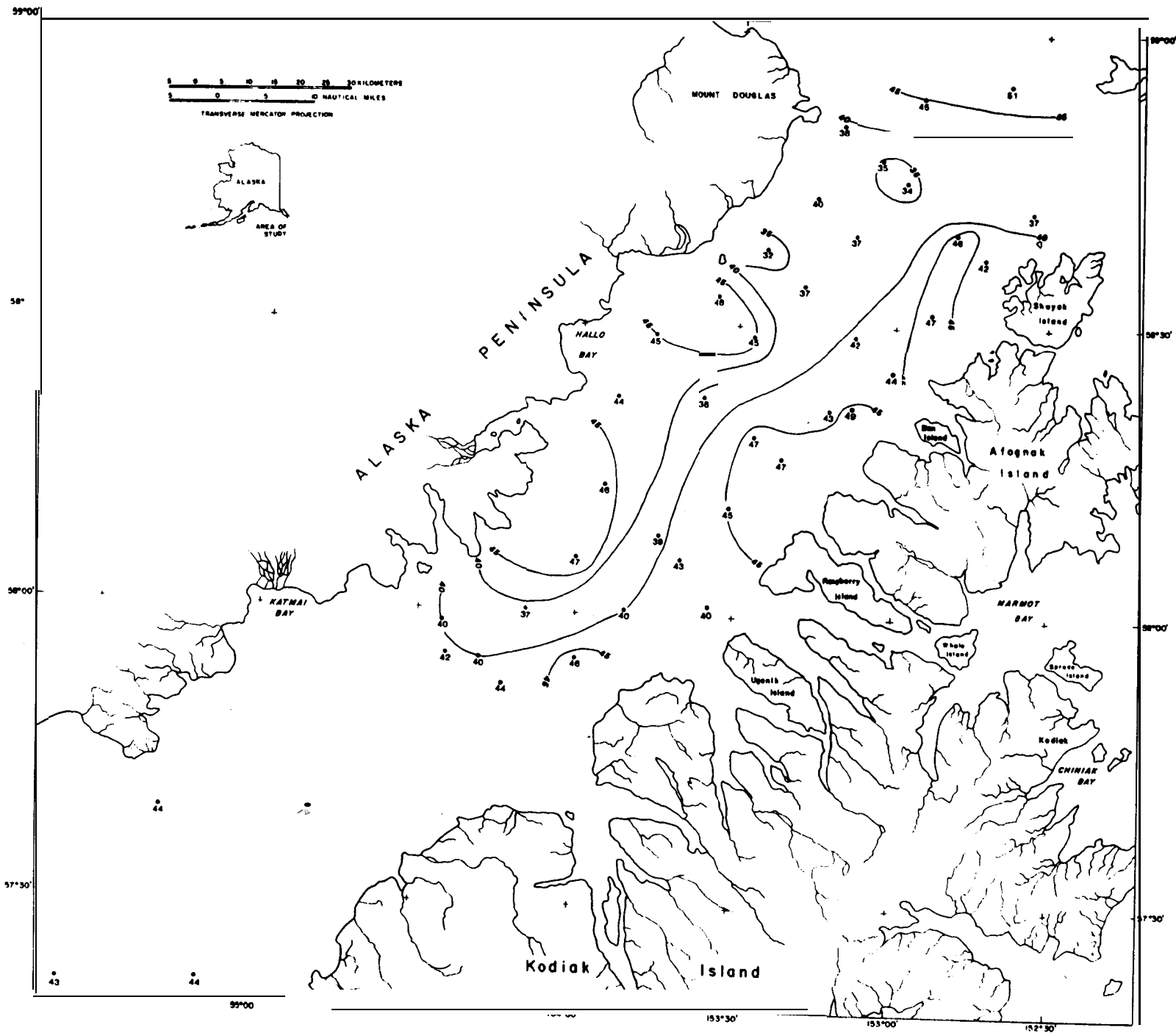


Fig. 30

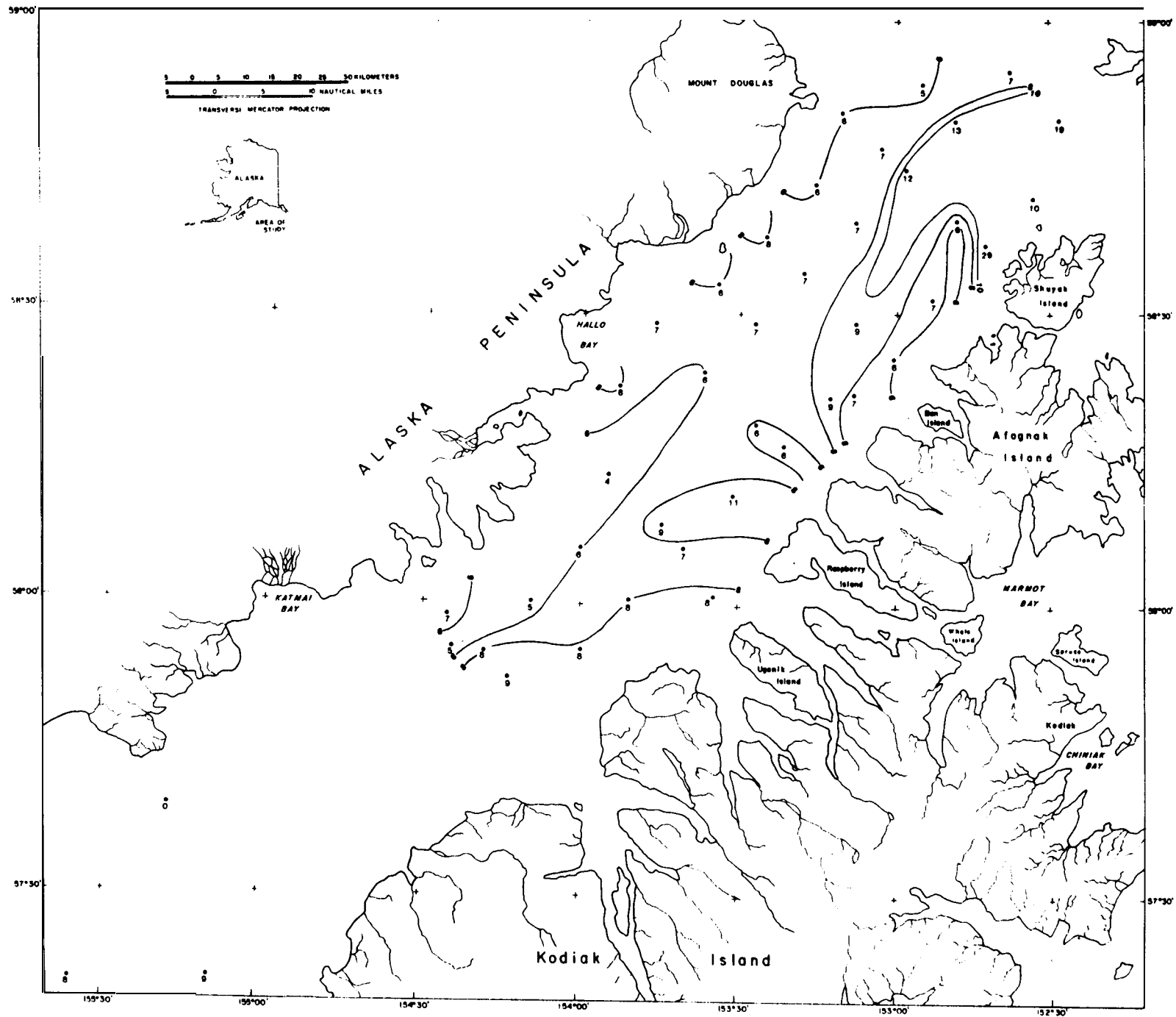


Fig. 31

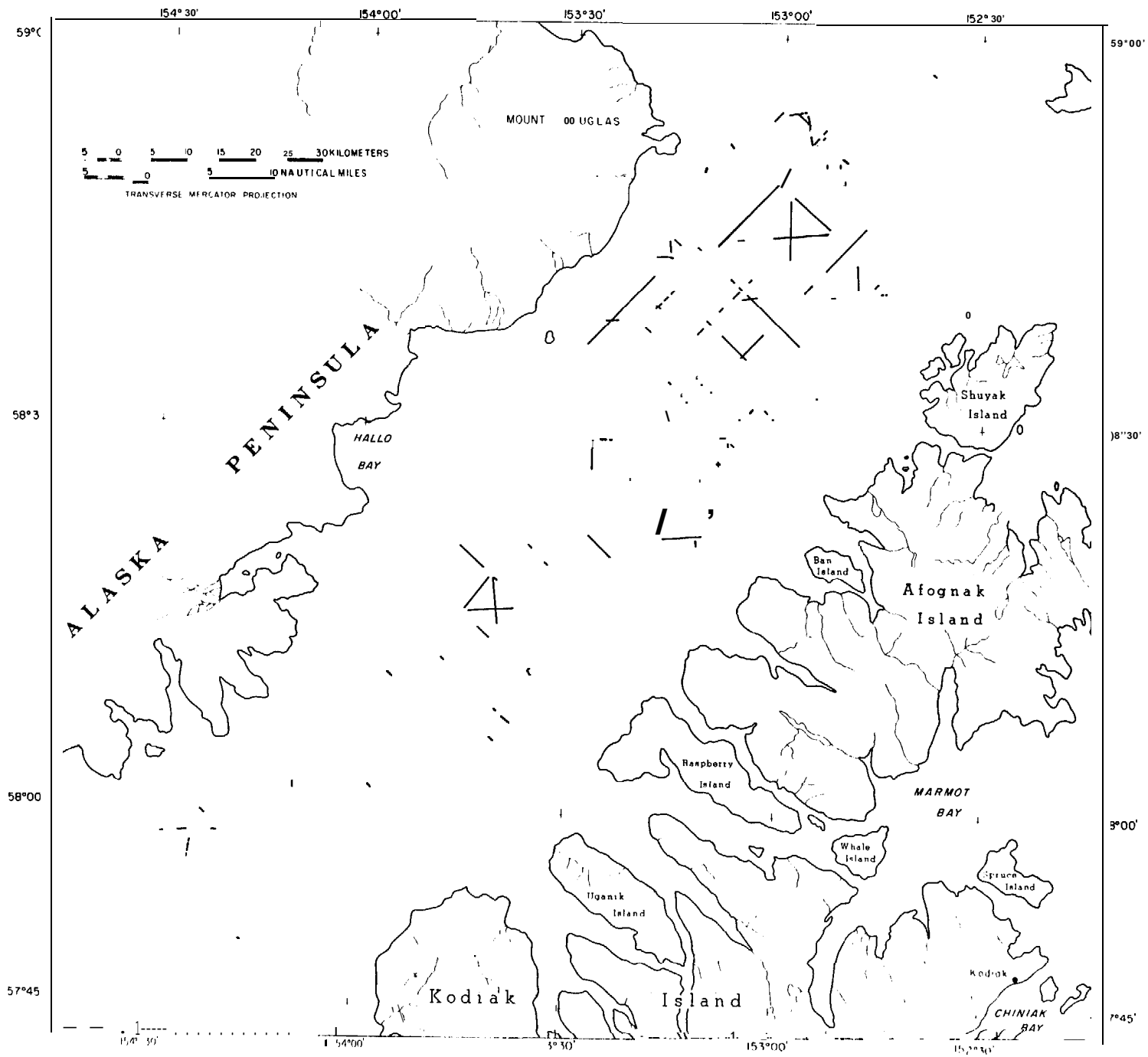


Fig. 52

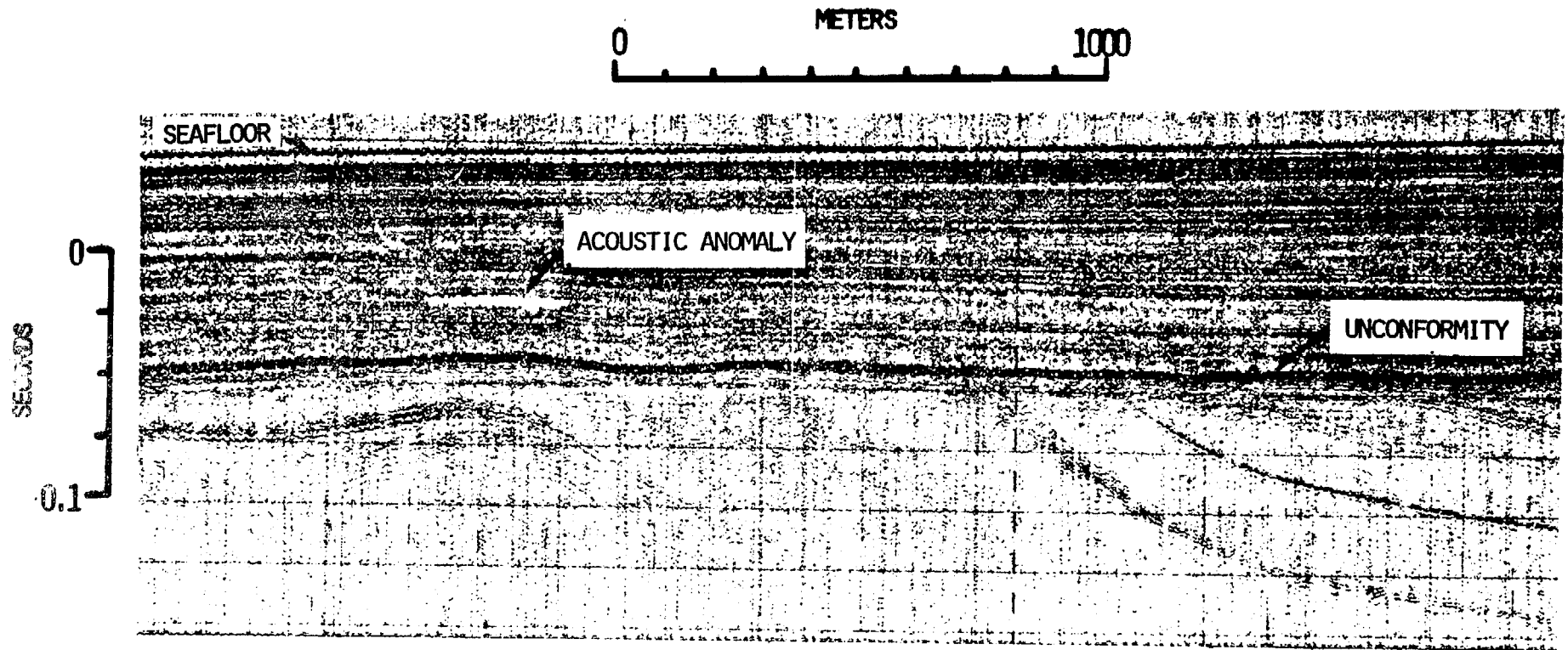


Fig. 33

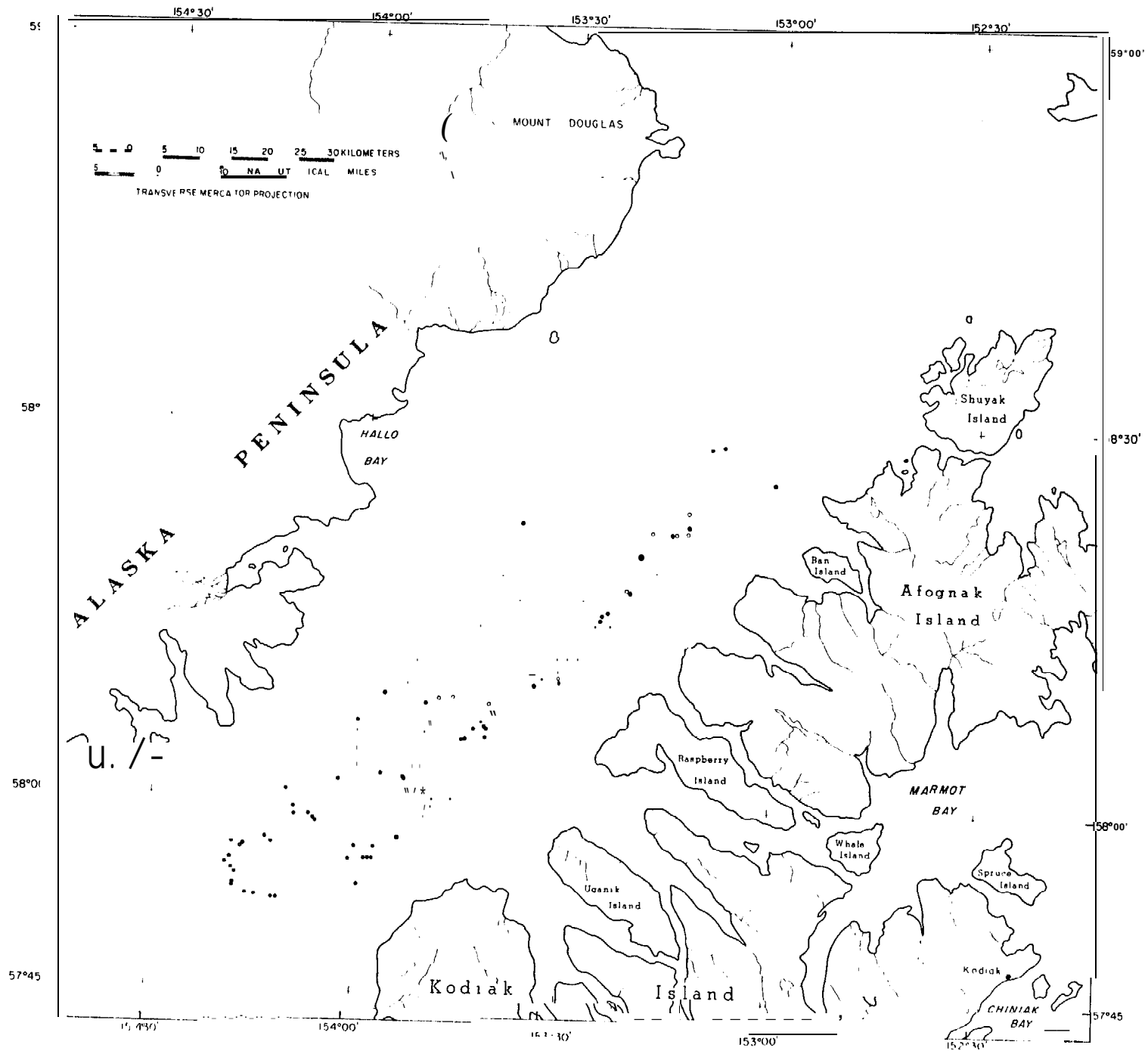


Fig. 04

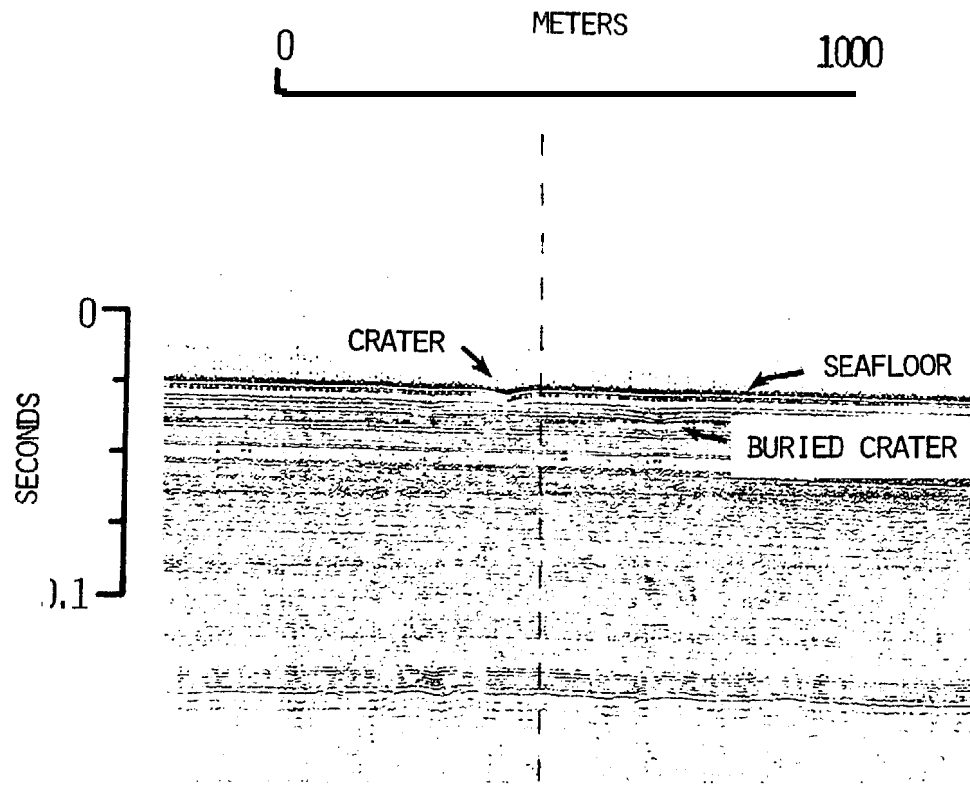


Fig. 35

